Thermal Evolution of a compositionally stratified Earth, including plates

by

Pieter Vermeesch

Submitted to the Department of Earth, Atmospheric, and Planetary Sciences
in partial fulfillment of the requirements for the degree of

Master of Science

at the

MASSACHUSETTS INSTITUTE OF TECHNOLOGY

May 2000
[June 2000]

Author .....
Department of Earth, Atmospheric, and Planetary Sciences
May 18, 2000

Certified by.....
Bradford H. Hager
Cecil and Ida Green Professor of Earth Sciences
Thesis Supervisor

Accepted by..
Ronald G. Prinn
Department Head

Thermal Evolution of a compositionally stratified Earth, including plates

by

Pieter Vermeesch

Submitted to the Department of Earth, Atmospheric, and Planetary Sciences
on May 18, 2000, in partial fulfillment of the
requirements for the degree of
Master of Science

Abstract

For subduction to occur, plates must bend and slide past overriding plates along fault zones. This deformation is associated with significant energy dissipation, which changes the energy balance of mantle convection and influences the thermal history of the Earth. To parameterize these effects, a subduction zone was included in a small region of a finite element model for the mantle, which also features an asthenosphere and a mid-oceanic ridge. Velocity boundary conditions were imposed in the vicinity of the subduction zone and a rate for subduction was specified, that balances the energy budget for convection. This balance includes an expression for the energy needed to bend the oceanic lithosphere as it subducts. Four different modes of energy dissipation were considered: viscous bending, brittle bending, viscous simple shear, and brittle simple shear.

We present theoretical arguments for, and numerical illustrations of the fact that for most modes of deformation, the simple powerlaw relationship of parameterized convection $Nu \sim Ra^{\beta}$ is not valid anymore, although it is still a good first order approximation. In the case of viscous bending dissipation and non-depth dependent brittle simple shear however, $Nu \sim Ra^{\beta}$ does hold. β is less than the value of $1/3$ predicted by standard boundary layer theory. For viscous energy dissipation, two different regimes of mantle convection can be considered, depending on the effective viscosity of the lithosphere: the "mobile lid" regime, and the "stagnant lid" regime. For brittle dissipation, the lithosphere strength is a function of yield stress which, when nearing a certain critical value, introduces a third regime, that of the "episodic overturning". Within the "mobile lid" regime, the plate velocities for models with a subduction zone governed by brittle behavior are far less dependent on the plate stress than those models with viscous deformation. This suggests that the plate motion is resisted by viscous stresses in the mantle.

The "mobile lid" would be representative for mantle convection associated with plate tectonics, as we observe on Earth. A "stagnant lid" would be the case for the Moon

or Mars, while Venus could experience the "episodic overturn" regime featuring cyclic and catastrophic brittle mobilization of a lithosphere with high friction coefficient.

Thesis Supervisor: Bradford H. Hager
Title: Cecil and Ida Green Professor of Earth Sciences

Acknowledgments

In the first place, I would like to acknowledge Brad Hager, my thesis advisor and Geosystems coordinator, who suggested to me this topic which I enjoyed studying very much. I cannot thank enough Clint Conrad, whose Ph.D. thesis work "Effects of Lithospheric Strength on Convection in the Earth's Mantle" was the firm basis for this Master's thesis. He helped me out whenever I had a problem with ConMan, or with anything else. His respose from Caltech always came very promptly, thanks to the marvel of e-mail. Maybe I should hence also thank the people that made the Internet! Many thanks to my Geosystems colleagues Lorraine, Russ, Chris, and Victoria for the fantastic year I had with them @ MIT. Good luck to you all!

This work was performed while being a recipient of a Francqui Fellowship of the Belgian American Educational Foundation.
Partial financial support was provided by NSF grant EAR-9905779.

Contents

Chapter 1

Introduction

Understanding of Earth's thermal history yields a better understanding of its structure and composition. The more realistic model of heat transfer proposed here should contribute to this discussion. The heat flux that is measured at the Earth's surface has two main sources. The first component is remnant heat of previous stages in the Earth's thermal history, beginning with its accretion 4.6 Ga BP. The second component is that of the present day heat production by radioactive decay of mainly U, Th, and K. There are three mechanisms by which the Earth cools down. The first two mechanisms are conduction and convection. The mantle can be treated as a Rayleigh-Bénard fluid which is heated from below and cooled from the top. This causes density differences which drive mantle convection. At the top and the bottom of the convection cell, two thermal boundary layers are formed. The cold, and stiff upper boundary layer is called the lithosphere and will be defined by a temperature of 1400K. Through the lithosphere, conduction is the main mechanism of heat transport. The third, and last mechanism of heat transport is radiation. We will neglect this component in our discussion, since the surface temperature of our planet is too low to give rise to black body radiation of any significance, compared with the two other mechanisms of heat dissipation.

The motion of Earth's tectonic plates are the surface expression of mantle convection. Because the plates form a cold boundary layer, they are denser than the mantle beneath them, and thus gravitationally unstable. Gravitational instability

results in the subduction of oceanic lithosphere [*Turcotte and Oxburgh,* 1967]. Nearly all previous studies of the thermal evolution of our planet have been based on this boundary-layer theory applied to a mantle with uniform composition. The Rayleigh number determines the vigor of convection, and is inversely proportional to the viscosity, while the Nusselt number Nu is a measure for the global efficiency of convective heat transport. In the traditional theory of "parameterized convection", a simple relation between the Ra and Nu is used: $Nu \propto Ra^{\beta}$. β is the key parameter in the theory of parameterized convection, and boundary layer theory predicts it to have a value of 1/3. This simple parameterization allows us to estimate the Earth's efficiency of cooling and the evolution of its temperature with time. It represents a self-regulating mechanism which strongly couples the heat loss and the internal temperature of the Earth. However, such a simple model of Earth's thermal history does not reconcile an apparent discrepancy between the observed surface heat flux and the heat production of the mid-ocean ridge basalt (MORB) source region: the two suggest a present day rate of heat production that is less than 50% of the present rate of heat loss [*Kellogg et al.,* 1999]. This means that more than 50% of the Earth's heat loss could be accounted for by secular cooling from a previous, hotter stage. This would suggest that Earth is very inefficient in dissipating its internal heat. Since heat production was exponentially higher in the past, this observation yields unrealistic models of Earth's thermal history when isoviscous boundary layer theory is applied. Because of the increase of the importance of convection with time, plate velocities would be unrealistically high in the Archaean [*Christensen,* 1985]. A lot of the discussion in this thesis will be concerned with whether or not we can still use the simple powerlaw equation of parameterized convection if we introduced some complications to the model, and what the value of β would be in that case.

Recent work at MIT resulted in two modified versions of boundary layer theory. In a first approach, the mantle is regarded as two compositionally distinct layers. The upper layer corresponds to a depleted MORB source. The deeper layer would then have a higher content of U, Th and K and, thus, account for some of the missing radioactive heat [*Kellogg et al.,* 1999]. This would decrease the importance of the

experimentally determined deficiency of radioactive heat production.

A second approach considers the effect of temperature dependent mantle viscosity on the bending resistance of subducting lithosphere. One simplification that standard boundary layer theory makes is that the mantle has an isoviscous rheology. In reality, the cold temperatures of the lithosphere make is exponentially stiffer than the underlying mantle, a fact that makes plates move as rigid units. Laboratory measurements suggest an order of magnitude variation in viscosity for every 100^oC of temperature change [*Kohlstedt,* 1995]. The temperature dependence of viscosity thus strengthens the interior of lithospheric plates. It should however also strengthen subduction zones. The temperature gradients across the ductile part of the lithosphere are several hundreds ^oC large. This should be enough to "freeze" plates and develop a "stagnant lid" regime of mantle convection, but this situation is not observed on Earth. Hence, a weakening mechanism is required to allow the lithosphere of deforming at subduction zones. This mechanism is not well understood. Brittle failure and viscous flow are the two ways by which materials can deform. This deformation dissipates energy. The resistance of the cold lithosphere to its deformation at subduction zones slows down convection and, thus, weakens the efficiency of cooling. This fenomenon diminished the degree of coupling between heat flow and mantle temperatures and reproduces more realistic Archaean plate velocities.

Deformation at subduction zones has been studied in localized high resolution finite element models [e.g. *Conrad and Hager*, 1999a]. In such models, the main deformation is associated with the bending and unbending of the slab, and so is the energy dissipation, which can take up to 30% of the mantle's total convective resistance [*Conrad*, 2000]. In order to model the effect of energy dissipative subduction zones on global scale mantle convection, we cannot use such a high resolution approach. Due to computational constraints, the deformation of the lithosphere has to take place in only a few elements of a regularly spaced grid. To solve this problem, an expression can be derived for the viscous dissipation associated with bending of a plate as a function of the plate velocity. A finite element model then parameterizes subduction dissipation by specifying velocity boundary conditions that force the litho-

sphere in a subduction-like geometry and balance the mantle's total energy budget, which includes the subduction dissipation. Using this approach, a finite element code called "SubMan" was used by *Conrad* [2000] to model bending dissipation by a plate with viscous rheology. It was assumed that all deformation can be represented by one "effective viscosity". In reality, the deformation happens through a complicated interaction of pure shear and simple shear, and rheologies ranging between the end members of viscous flow and brittle/ductile flow. Brittle behavior of subduction zones is supported by clear experimental evidence. In fact, a major part of the seismicity on our planet is confined to these subduction zones.

In this thesis, I will describe how a modified version of SubMan can be used to model modes of energy dissipation other than viscous flow under pure bending strain. Thus, to make subduction dynamically self-consistent, we specify a rate at which subduction occurs by applying an energy balance for the mantle. This balance includes an equation for the energy dissipated at the subduction zone. In order to model brittle deformation, this equation will include a yield stress. So far, we have looked only at plates deforming under bending shear. However, this is not the only strain pattern under which subduction can occur. Two more energy dissipation equations will be derived for the case of simple shearing deformation, again for both viscous and brittle rheology. This brings the total number of suduction modes to four. Each of these modes corresponds to an equation for the energy dissipation that is a different function of the plate velocity, the plate thickness, and the effective viscosity or -for brittle behavior- two yield stress parameter.

I will first show that the new code successfully incorporates the original SubMan model, by repeating the numerical experiments done by *Conrad,* [2000] for viscous dissipation under pure bending. Next, similar experiments will be carried out for the other three modes of deformation. Finally, the results of numerical experiments will be critically evaluated for their consequences regarding boundary layer theory and the reconstruction of the thermal history of the Earth. The four modes of deformation here discussed correspond to the end members of stress/strain interaction. They should be considered constraints on real world situations.

Chapter 2

Background

The general formulation of Earth's thermal evolution can be written:

$$\frac{d}{dt}\int_V \rho C_p T dV = \int_V H dV - \int_S F dS \tag{2.1}$$

Where t is time, V is the volume of the earth, S its surface area, ρ is density, C_p is specific heat, T is temperature, H is the rate of radiogenic heating and F is the surface heat flux. For given values of C_p, ρ, and H, this equation gives us T as a function of F. Most of the research on Earth's thermal history is concerned with determining this function [*Richter,* 1984], and so is the research proposed here. First we define the Nusselt number Nu, which is the ratio of the total surface heat flow Q to the hypothetical heat flow $Q_{cond}(\bar{T})$ which would occur if the only mechanism of heat loss was conduction [*Christensen,* 1985]:

$$Nu \equiv \frac{Q}{Q_{cond}(\bar{T})} = \frac{Q}{c\bar{T}} \tag{2.2}$$

where $\bar{T}$ is the average temperature of the convection cell and c is a factor depending on the mode of heating. Next we define the Rayleigh number Ra_m as:

$$Ra \equiv \frac{\alpha g \rho \bar{T} D^3}{\kappa \eta_m} \tag{2.3}$$

where α is the thermal expansivity, ρ the density, κ the thermal diffusivity, g the gravitational acceleration, D the system's depth and η_m the mantle viscosity. In general, the viscosity η strongly depends on the temperature T:

$$\eta(T) = \eta_m exp\left(\frac{E_a}{RT} - \frac{E_a}{RT_m}\right) \tag{2.4}$$

where E_a is the activation energy, T_m is the mantle temperature and R is the universal gas constant [*Kohlstedt et al.,* 1995]. Both boundary-layer theory and experiments have shown that there is an exponential relationship between the Rayleigh and the Nusselt number, which characterizes the convective system [e.g. *Turcotte and Oxburgh,* 1967]:

$$Nu \propto Ra_m^{\beta} \tag{2.5}$$

where β is the parameter in the theories of parameterized convection [e.g. *Christensen,* 1985, *Davies,* 1980, *Conrad and Hager,* 1999b]. Since Nu is a measure of Earth's surface heat flux (F) and Ra_m is a function of the temperature (T), this equation relates T and F. For a system with constant viscosity and constant basal temperature, boundary layer theory gives a parameter value $\beta = 1/3$ [*Turcotte and Oxburgh,* 1967]. We can now use (2.5) to solve (2.1), which will then give us the evolution of temperature or surface heat flow with time.

When the temperature of the mantle is high, viscosity will be low, and thus, Ra_m will be high. A high value for β - such as 1/3 - will also result in a high Nu, and thus an efficient rate of convective cooling. Cooling of the mantle will then cause the viscosity to increase (equation (2.4)). By definition (equation (2.3), Ra_m

will therefore decrease and because of (2.5), Nu will decrease. The rate of cooling will then slow down. This negative feedback mechanism results in a buffering of the mantle temperature over Earth's history. By this mechanism, Earth will reach a state of thermal stability, with a ratio of heat production to heat dissipation near unity. We will call this ratio the Urey ratio [*Christensen,* 1985]. Boundary-layer theory with β equal to 1/3 predicts a Urey ratio of 0.85. This means that less than 15% of the present day heat flow would be the result of secular cooling of the Earth's mantle of an initially hotter state. Total heat loss was however considerably higher in the past due to higher heat production. Using the rule that the heat loss by seafloor spreading is proportional to the square of the plate velocity, one can calculate the average plate velocity during time. For β equal to 1/3, this would result in unrealistically high Archaean mid-ocean ridge spreading rates [*Christensen,* 1985].

If the mantle had the same composition as MORBs, mantle heat production would only be 2 to 6TW [*Kellogg et al.,* 1999]. With a total terrestrial heat flow of 44 TW, these low values of mantle heat production imply a Urey ratio of only 0.06 [Conrad and Hager, 1999a & b]. In order to keep β high and thus preserve the negative feedback mechanism for the temperature of the mantle, a higher mantle heat production is required. Geochemical models of the Earth based on an initial average composition of chondritic meteorites imply a current mantle heat production of 15TW [*Jochem et al.,* 1983]. There must thus be an extra heat source apart from the MORB source. Seismological evidence and the isotopic signatures of oceanic island basalts suggest the existence of a compositionally distinct layer in the deep mantle [*Kellogg et al.,* 1999]. When we include this layer in the geochemistry of the mantle, the Urey ratio increases to a maximum value of 0.60. This ten times higher than the value which we have shown to be predicted by a mantle of uniform composition. 0.60 is, however, still significantly less than the Urey ratio of 0.85 predicted by standard boundary-layer theory.

To allow Urey ratios of less than 0.85 without violating the geochemical models for the Earth, we must use another approach, and allow β to be smaller than 1/3. We should therefore modify isoviscous boundary-layer theory in order to weaken the

negative feedback mechanism that stabilizes mantle temperatures. The rate of convection of the mantle should respond less effectively to changes in the temperature of the mantle. There must thus exist a force which is stronger than the resistance against deformation of an isoviscous mantle. *Christensen* (1985) states that it is not the viscosity of the bulk of the convecting fluid that controls heat transfer, but rather the properties of the cool and exponentially stiffer top boundary layer. This stiff rheology will resist deformation at subduction zones by viscous dissipation and brittle behavior. *Conrad* (2000) modeled this concept numerically by including a subduction zone in the finite element code ConMan [*King et al.*, 1990].

The energy balance of the convective system is [*Conrad and Hager,* 1999b]:

$$\Phi^{pe} = \Phi_m^{vd} + \Phi_l \tag{2.6}$$

with Φ^{pe} = the total potential energy released, Φ_m^{vd} = the viscous dissipation in the mantle, and Φ_l = the energy dissipation associated with bending of the lithosphere in the subduction zone. In a first approach, the entire bulk of energy dissipation within the subduction zone is presumed to be caused by viscous bending resistance. One can show that [*Conrad and Hager,* 1999a]:

$$\Phi^{pe} = \frac{\rho g \alpha \triangle l_s h_s}{\sqrt{\pi}} v_p = C_{pe} v_p \tag{2.7}$$

$$\Phi_m^{vd} = C_m v_p^2 \eta_m \tag{2.8}$$

where ρ is density, g is the gravitational acceleration, α is the thermal expansivity, $\triangle T = T_{int} - T_s$ is the temperature difference between the interior of the mantle and the surface, l_s is the length of the subducted portion of the slab, h_s is the thickness of the slab at the subduction zone, C_m is a constant, v_p is the plate velocity,

and η_m is the viscosity of the mantle. The viscous energy dissipation associated with the deformation of a continuum can be written as [*Chandrasekhar,* 1961]:

$$\Phi = \int_V \tau_{ij} \dot{\epsilon_{ij}} dV \tag{2.9}$$

where τ_{ij} is the stress tensor, and $\dot{\epsilon_{ij}}$ is the strain rate given by:

$$\dot{\epsilon_{ij}} = \frac{1}{2}\left(\frac{\partial u_i}{\partial x_j} + \frac{\partial u_j}{\partial x_i}\right) \tag{2.10}$$

When the continuum is an incompressible fluid with an "effective viscosity" η :

$$\tau_{ij} = 2\eta \dot{\epsilon_{ij}} \tag{2.11}$$

and (2.9) becomes:

$$\Phi^{vd} = 2\int_V \eta \dot{\epsilon_{ij}} \dot{\epsilon_{ij}} dV \tag{2.12}$$

In the case of bending resistance by viscous flow, the horizontal strain ϵ_{xx} associated with bending is equal to the change of length of a fiber l_c in the curved part of the slab:

$$\epsilon_{xx} = \frac{\Delta l_c}{l_c} = \frac{y}{R} \tag{2.13}$$

where v_p is the plate velocity, y is the distance from the centerline of the bended slab, and R is the slab's radius of curvature. Since l_c is proportional to R (see figure 3.2) we can now write for the strainrate:

$$\dot{\epsilon_{xx}} = \frac{2}{\pi}\frac{v_p}{R}\frac{y}{R} \tag{2.14}$$

Plugging (2.14) in (2.12) yields [*Conrad and Hager,* 1999]:

$$\Phi_l^{vd} = C_l v_p^2 \eta_l \left(\frac{h_s}{R}\right)^3 \tag{2.15}$$

where η_l is the viscosity of the lithosphere, R is the subduction zone's radius of curvature and C_l is a constant which incorporates all constants of proportionality and integration that arise in the derivation. *Conrad and Hager* (1999a) find a value of 2 for C_l by simulating subduction in a high resolution finite element grid. The analytic solution of the integration yields a value of $C_l = \frac{1}{3\pi}$. The difference between these two values is due to the fact that temperature-dependent viscosity is used, as defined in (2.4). Thus, viscosity changes throughout the bending plate, and it is strongest near the top of the plate (the coldest part). We also assumed that the viscous dissipation is constant along bands that are a uniform distance from the center of the bending slab. Numerical experiments clearly show that this is not true. The viscous dissipation is concentrated in bending and unbending zones [*Conrad and Hager,* (1999a)]. In order to compare the energy equation (2.15) for viscous behavior with the equations for brittle deformation that we will later derive, we will use the value of $C_l = \frac{1}{3\pi}$. We will then transfer any uncertainty in C_l into uncertainty in η_l.

It is found that up to 30% of the mantle's total convective resistance is associated with deformation occuring within the subduction zone [*Conrad,* 2000]. The extra resistance accounted for in this model allows β to be smaller than 1/3 and the Urey ratio to be smaller than 0.85. From (2.4), we know that η_l is a function of the temperature at the Earth's surface, which is believed not to have varied much since the Archaean, compared to the changes in mantle temperature. With equation (2.15), this then infers less variation of v_p with time than in the case of isoviscous boundary layer theory, where Φ_l^{vd} was not considered.

The model of a layered mantle yields a Urey ratio of 0.6 without requiring β to be smaller than 1/3. Models which include bending resistance at subduction zones allow the Urey ratio to be smaller than the 0.85 predicted by isoviscous boundary layer theory, but also infer a lower value of β. A combination of these two kinds of models could explain the present day observed heat flow, and allow us to reconstruct the Earth's thermal history with realistic plate velocities, i.e. approximately constant over time.

Chapter 3

Methods

3.1 The finite element code SubMan

The finite element program ConMan has been developed to model processes of mantle convection in two dimensions [*King et al.*, 1990]. The initial version of ConMan could simulate such phenomena as non-Newtonian viscosity and radioactive heat production. A recent version of the program called SubMan also includes a subduction zone [*Conrad,* 2000]. The energy dissipation associated with the bending of lithosphere with high viscosity in the subduction zone has been implemented in SubMan through equation (2.15) [*Conrad,* 2000]. It is the goal of this research to find equations that describe the energy dissipation resulting from brittle deformation of the subducting slab and use them to replace (2.15) in SubMan. I give only a brief introduction to the finite element method as applied to mantle convection and refer to *Hughes* (1987) and *Nikishkov* (1998) for futher reading about the subject.

The finite element method is a numerical technique for solving problems that are described by partial differential equations. Suppose that we need to numerically solve the following differential equation:

$$u_{,xx}(x) + f(x) = 0 \tag{3.1}$$

given f(x):[0,2L] $\rightarrow \Re$ and constants g and h, with boundary conditions u(2L)=g and $-u_{,x}(0) = h$. Equation (3.1) is called the strong form of the problem. In order to solve the differential equation numerically, the finite element method transforms it into an integral equation. We do this by multiplying (3.1) with a shape function w(x), where $w(2L) = 0$. This yields, after partial integration:

$$\int_0^{2L} w_{,x}(x)u_{,x}(x) \; = \int_0^{2L} w(x)f(x)dx \; + w(0)h \tag{3.2}$$

This is the weak formulation of the problem. If we consider a one-dimensional domain divided into two finite elements (figure 3-1.a), an example of a shape function for one element in this problem would be (figure 3-1.b)

$$w(x) = \left[1 - \frac{x - x_1}{x_2 - x_1}, \frac{x - x_1}{x_2 - x_1}\right] \tag{3.3}$$

so that we can approximate u(x) in the local element i as:

$$u(x) = w(x)u^i \tag{3.4}$$

where

$$u^i = [u1, u2] \tag{3.5}$$

Here u1 and u2 are the exact solutions of the equation at the nodal points of finite element i, which should be determined from the discrete global equation system. The local version of (3.2) for element i now is:

$$\int_{x_1}^{x_2} w_{,x}(x)u^i_{,x}(x)dx \ = \int_{x_1}^{x_2} w(x)f^i(x)dx \ + w(x_1)u^i_{,x}(x_1) \tag{3.6}$$

We integrate (3.6) for each element in the domain and add the results. We can now write (3.2) as a large sparse matrix equation:

$$[K]u = b \tag{3.7}$$

We call K the stiffness matrix and b the forcing vector. We have transformed the partial differential equation (3.1) into a simple linear algebra problem which is to be solved for u. It is the transformation between the local domain (3.6) and the global domain (3.2) that makes the finite element method so powerful. Although we make a very rough, piecewise-linear approximation to the function of interest, we can increase precision to any desired level simply by increasing grid density. This is illustrated for the case of f(x)=1 by figure (3-2). Incompressible mantle convection can be described by the equations of momentum:

$$\nabla(\eta\dot{\epsilon}) = \nabla p - \rho g \alpha \triangle T \hat{k} \tag{3.8}$$

continuity:

$$\nabla \cdot u = 0 \tag{3.9}$$

and energy:

$$\frac{\partial T}{\partial t} = \kappa \nabla^2 T - u \cdot \nabla T + H \tag{3.10}$$

where η is the viscosity, $\dot{\epsilon}$ is the strain rate, p pressure, ρ density, g the gravitational acceleration, α the thermal expansion coefficient, T temperature, $\hat{k}$ is the unit vector in the vertical direction, u is the velocity, t time, and H is a heat source term [e.g., *Chandrasekhar*, 1961; *Turcotte and Oxburgh,* 1967]. We treat the incompressibility equation (3.9) as a constraint on the momentum equation and enforce incompressibility in the solution of the momentum equation using a penalty formulation [*Temam,* 1977, cited in *King et al.,* 1990]. Since temperature gradients produce the buoyancy forces that drive the momentum equation, the algorithm to solve the system is a simple one: first, given an initial temperature field, we calculate the resulting velocity field. We then use the velocities to advect the temperatures for the next time step and solve for a new temperature field [*King et al.,* 1990].

The momentum equation is solved through an approach similar to what is named the Galerkin method, which was described above [*Hughes,* 1987]. Weighting functions for the energy equation however are now given by a Petrov-Galerkin function [*King et al.,* 1990]. This method can be thought of as a standard Galerkin method in which we counterbalance numerical underdiffusion by adding an artificial diffusivity. The resulting matrix equation (3.7) is not symmetric. We however use an explicit time stepping method, and therefore the energy equation is not implemented in matrix form.

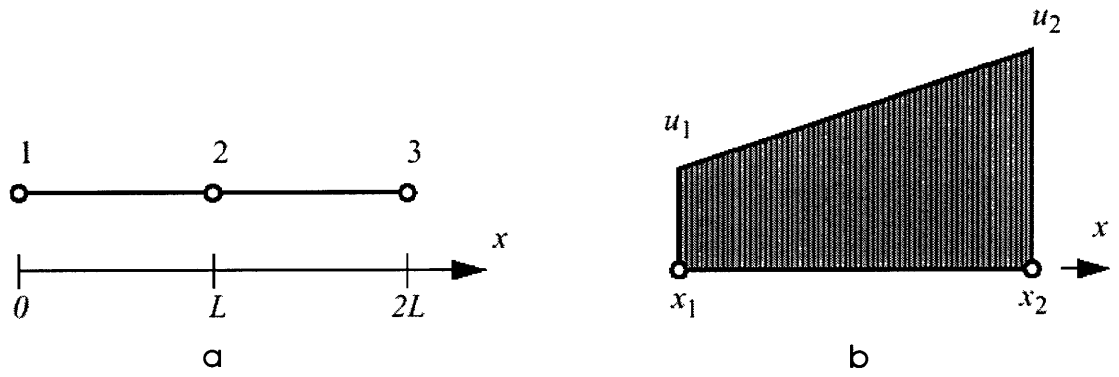

Figure 3-1: (a) One-dimensional domain divided into two finite elements, (b) Function approximation in one-dimensional element [from *Nikishkov,* 1998]

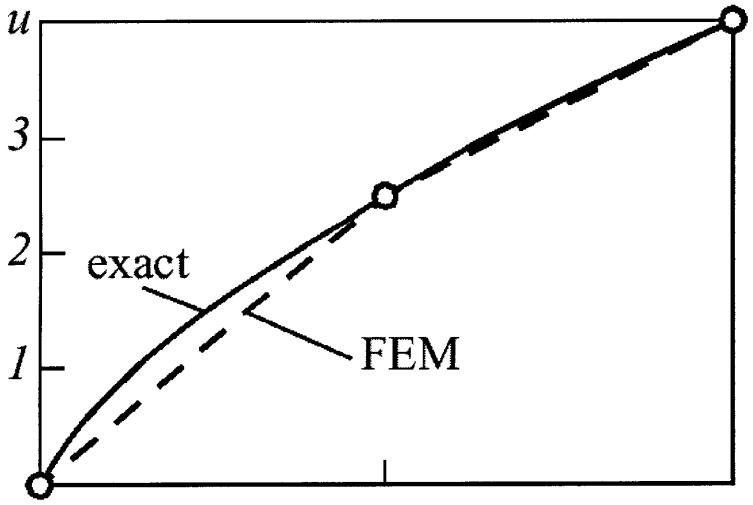

Figure 3-2: Exact solution of the differential equation (3.1) for f(x)=1 and finite element approximation (FEM) [from *Nikishkov,* 1998]

3.2 Brittle deformation of a slab under pure bending deformation

It is our goal to find an equation describing the energy dissipation associated with the brittle deformation of a subducting lithospheric plate and introduce this equation into the finite element code SubMan. In order to model the brittle behaviour of a subducting lithosphere, we will follow a strategy proposed by *Moresi and Solomatov* (1998). We assume that the collective behavior of a large set of randomly oriented faults can be described by a plastic flow law, and that it is not necessary to resolve individual faults. We introduce the concept of a yield stress τ_{yield} via the Byerlee yield criterion:

$$\tau_{yield} = c_0 + \mu\rho g z \tag{3.11}$$

where c_0 is a yield stress at zero hydrostatic pressure, μ is a frictional coefficient, ρ is density, g is the gravitational acceleration, and z is depth.

We can nondimensionalize this according to *Moresi and Solomatov* (1998):

$$\tau'_{yield} = \tau_0 + \tau_1 z' \quad , \tag{3.12}$$

where $z' = \frac{z}{D}$ is the nondimensionalized depth, with D = the thickness of the mantle layer. The non-dimensional cohesion term τ_0 is given by

$$\tau_0 = \frac{c_0 d^2}{\kappa \eta_0} \quad , \tag{3.13}$$

and the non-dimensional depth-dependent term of yield stress τ_1 is defined as

$$\tau_1 = \frac{\mu Ra_0}{\alpha \Delta T} \tag{3.14}$$

Other non-dimensional quantities we will use are time and distance

$$t' = t\frac{\kappa}{D^2} \qquad and \qquad x' = \frac{x}{D} \quad , \tag{3.15}$$

with κ = the diffusivity. Temperature is non-dimensionalized according to:

$$T' = \frac{T - T_s}{T_b - T_s} \quad , \tag{3.16}$$

where T_s is the surface temperature, and T_b the temperature at the grid base. For convenience, we will drop the primes denoting the non-dimensional nature of these quantities in future calculations. The deformation described above and modeled by *Conrad and Hager* (1999a) for viscous dissipation is essentially a bending deformation. We will in a first approach continue on this path and model the brittle behavior with the same straining conditions as used by *Conrad and Hager* (1999a). For our 2 dimensional problem, substituting (2.14) and (3.12) in (2.9) yields the following equation for the brittle energy dissipation of the bending lithosphere:

$$\Phi_l^{bd,ps} = \frac{2}{\pi} \int \int_S (\tau_0 + \tau_1 z) \frac{v_p \mid y \mid}{R^2} dS \quad , \tag{3.17}$$

where we take the absolute value of y to make the strain rate always positive. This was not necessary for the case of viscous bending dissipation because due to (2.11) the stress was proportional to the strainrate so that (2.9) was always positive. From the geometry of our problem as summarized in figure (3.3):

$$z = \left(R + \frac{h}{2}\right) - (R + y)\cos\theta \tag{3.18}$$

Plugging (3.18) in (3.17) yields:

$$\Phi_l^{bd,ps} = \int_{-\frac{h}{2}}^{\frac{h}{2}} \int_0^{\frac{\pi}{2}} (R + y)\left(\tau_0 + \tau_1\left(\left(R + \frac{h}{2}\right) - (R + y)\cos\theta\right)\right)\frac{v_p \mid y \mid}{R^2} d\theta \; dy \tag{3.19}$$

The solution of this integral is:

$$\Phi_l^{bd,ps} = \frac{1}{16\pi}\frac{v_p h^2\left(4\pi R\tau_0 + \left((4\pi - 8)R^2 + 2\pi hR - h^2\right)\tau_1\right)}{R^2} \tag{3.20}$$

When we compare this equation for the brittle energy dissipation with the equation describing viscous energy dissipation (2.15), we see that instead of a proportionality with v_p^2, we are now faced with a proportionality with v_p.

3.3 Deformation of a subducting slab under simple shear

Pure bending is not the only way by which plates can deform. The other way is by simple shear, as represented in figure (3.4). It is easily seen that the strain rate here is:

$$\dot{\epsilon} = \frac{v_p \tan(\gamma)}{w} \tag{3.21}$$

With w being the width of the subduction zone, and γ the angle of subduction. The energy dissipation of the deformation is still given by (2.9). For the case of viscous

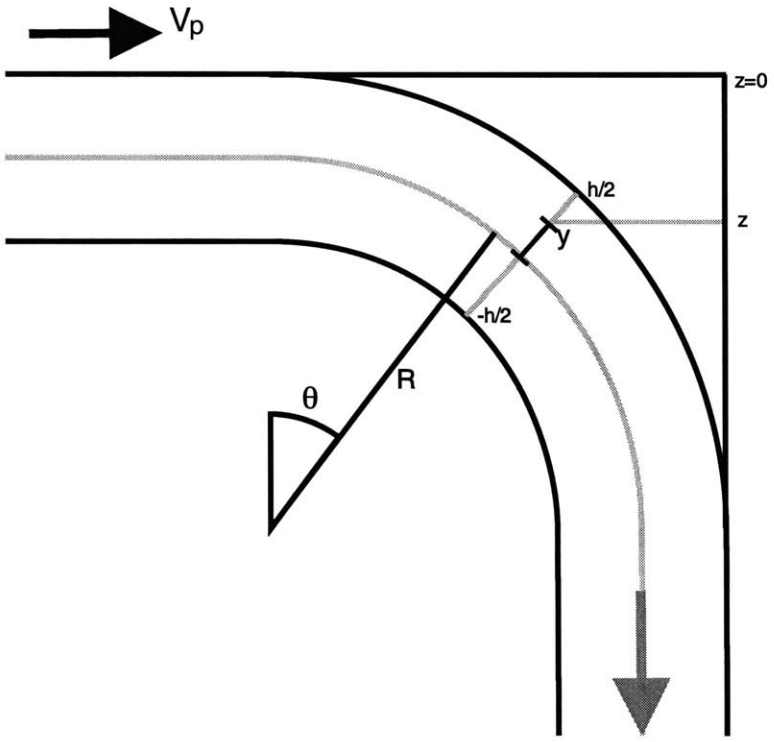

Figure 3-3: Subduction with pure bending dissipation geometry

rheology, this again simplifies to (2.12), which combines with (3.21) in:

$$\Phi_l^{vd,ss} = \frac{2\eta_l v_p^2 \tan(\gamma)^2 h}{w} \tag{3.22}$$

In the case of brittle deformation of a lithospheric slab deforming under simple shear, we use the general equation (2.9) with stress τ given by (3.12) and strainrate given by (3.21):

$$\Phi_l^{bd,ss} = \int_0^w \int_0^h (\tau_0 + \tau_1(x\tan(\gamma) + y)) \left(\frac{v_p \tan(\gamma)}{w}\right) dy\ dx \tag{3.23}$$

Solving this integral yields:

$$\Phi_l^{bd,ss} = h v_p \tan(\gamma) \left((\frac{\tau_1}{2} w \tan(\gamma) + \frac{\tau_1}{2} h + \tau_0\right) \tag{3.24}$$

The geometry of a single phase simple shearing deformation (figure (3.4)) is different from the geometry of bending dissipation (figure (3.3)). Therefore we cannot easily compare the two cases. We can however repeat the simple shearing various subsequent times. As shown by figure (3.5), this yields more realistic subduction geometries. The general formulation of viscous and brittle bending resistance with simple shear can now be written as:

$$\begin{aligned}\Phi_l^{vd,ss} &= \lim_{n\to\infty}\sum_{i=1}^{n}\int_0^{h_i}\int_0^{w_i} 2\eta_l\left(\frac{v_p\tan(\gamma)}{w_i}\right)^2 dxdy \\ &= \frac{\pi\, n_l\, v_p^2\, h}{R+\frac{h}{2}}\end{aligned} \tag{3.25}$$

$$\begin{aligned}\Phi_l^{bd,ss} &= \lim_{n\to\infty}\sum_{i=1}^{n}\int_0^{h_i}\int_0^{w_i} (\tau_0+\tau_1 z)\,\frac{v_p\tan(\gamma)}{w_i}dxdy \\ &= hv_p\left(\frac{\pi}{2}\tau_0+\left((\pi-1)\,\frac{h}{2}+\left(\frac{\pi}{2}-1\right)\left(R-\frac{h}{2}\right)\right)\tau_1\right)\end{aligned} \tag{3.26}$$

3.4 Implementation

To simulate mantle convection with energy dissipation by subduction zones, a finite element grid was set up according to the principles outlined in the beginning of this chapter. This grid with aspect ratio 1.5 has a resolution of 40 by 60 elements. Four different regions ("material groups") are distiguished by viscosity. For the mantle and subduction zone regions, viscosity is temperature dependent, according to (2.4). The subduction zone is 9 by 9 elements in size and situated in the upper right corner of the grid. A "ridge" is implemented in the upper left corner. It is 2 elements wide and 9 elements deep. The viscosity of the ridge is low and constant: $\eta_r = \eta_m(T=1)$. The fourth material group is an "asthenosphere". Situated from element 4 through 9 from the surface, it has a viscosity 10 times smaller than that of the mantle. Thus, it prevents the lithosphere of thickening too much when the subduction zone is strong. The location of the various material groups is illustrated by figure (3.6). To parameterize the deformation associated with subduction, velocity boundary conditions are imposed in the vicinity of the subduction zone. A rate of subduction is specified that balances the energy budget for convection. This includes an expression for the energy needed to bend the oceanic lithosphere as it subducts. The energy balance for mantle convection is given by (2.6). The velocity with which we force subduction is

calculated from the energy balance by an iterative procedure. In a first step, subduction is forced with a chosen velocity v_{i-1}, and Φ^m and Φ^{pe} are measured. The plate thickness h_p is estimated using the depth of the $T = T_{int}erf(1) = 0.55$ isotherm, which should correspond to the thickness of the thermal boundary layer. With these values , equation (2.7), and (2.8), we get a first estimate for C_{pe} and C_m. Applying these estimates to (2.6) yields an expression for v_i that depends on v_{i-1}. In the case of viscous behavior, where Φ_l is a function of v_p^2 (see (2.15) and (3.25)):

$$v_p = v_i = v_{i-1}\frac{\Phi^{pe}}{\Phi_m + \Phi_l} \tag{3.27}$$

This procedure is repeated until the imposed velocity does not change by more than 0.01%. For the case of brittle behavior (equations (3.20) and (3.21)), the energy dissipation is proportional to v_p, and the imposed subduction velocities are calculated with:

$$v_p = v_i = v_{i-1}\frac{\Phi^{pe} - \Phi_l}{\Phi_m} \tag{3.28}$$

To initiate subduction, we first impose a constant subduction velocity of v_i=500 on an initially isothermal mantle with temperature T_{int}=0.65 and Rayleigh number $Ra_m = 10^6$. The top of the mantle cools down and forms a lithosphere which subducts into the mantle, forming a slab. After a while, the temperature field ceases to change significantly with time. This temperature field is used as the initial condition in all further runs, which have dynamically chosen rates of subduction, as described above. The 4 modes of energy dissipation associated with subduction zones are summarized in table (3.1). In what follows, we will refer to the various ways through which subduction zones can dissipate energy with the terminology of mode1 through mode4 which is defined in this table.

mode	Φ_l	v_i
1	$\Phi_l^{vd} = \frac{1}{3\pi} v_p^2 \eta_l \left(\frac{h_s}{R}\right)^3$	$v_{i-1} \frac{\Phi^{pe}}{\Phi_m + \Phi_l}$
2	$\Phi_l^{bd,ps} = \frac{1}{16\pi} \frac{v_p h^2 \left(4\pi R \tau_0 + \left((4\pi - 8) R^2 + 2\pi h R - h^2\right) \tau_1\right)}{R^2}$	$v_{i-1} \frac{\Phi^{pe} - \Phi_l}{\Phi_m}$
3	$\Phi_l^{vd,ss} = \frac{\pi \eta_l v_p^2 h}{R + \frac{h}{2}}$	$v_{i-1} \frac{\Phi^{pe}}{\Phi_m + \Phi_l}$
4	$\Phi_l^{bd,ss} = h v_p \left(\frac{\pi}{2} \tau_0 + \left((\pi - 1) \frac{h}{2} + \left(\frac{\pi}{2} - 1\right) \left(R - \frac{h}{2}\right)\right) \tau_1\right)$	$v_{i-1} \frac{\Phi^{pe} - \Phi_l}{\Phi_m}$

Table 3.1: model = viscous bending dissipation (2.15), 2 = brittle bending dissipation (3.20), 3 = Simple shear viscous dissipation (3.25), and 4 = Simple shear brittle dissipation (3.26)

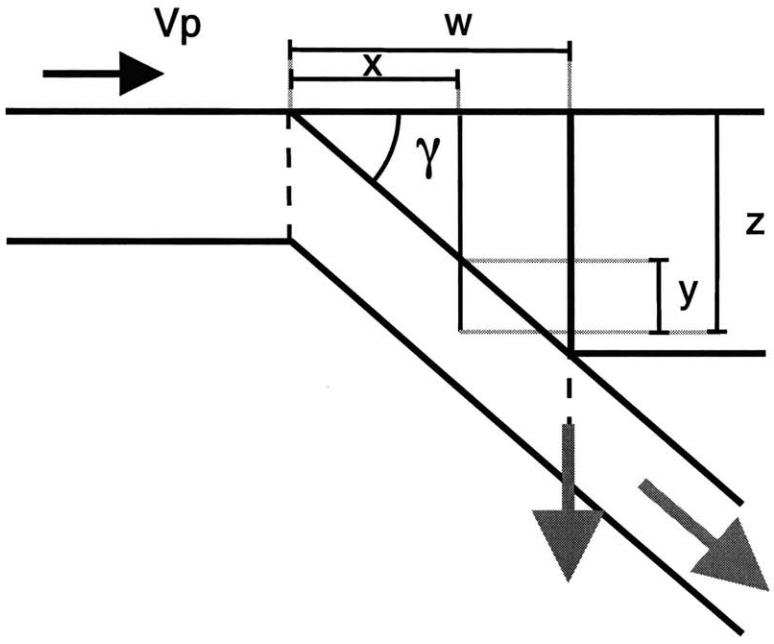

Figure 3-4: Subduction under simple shear.

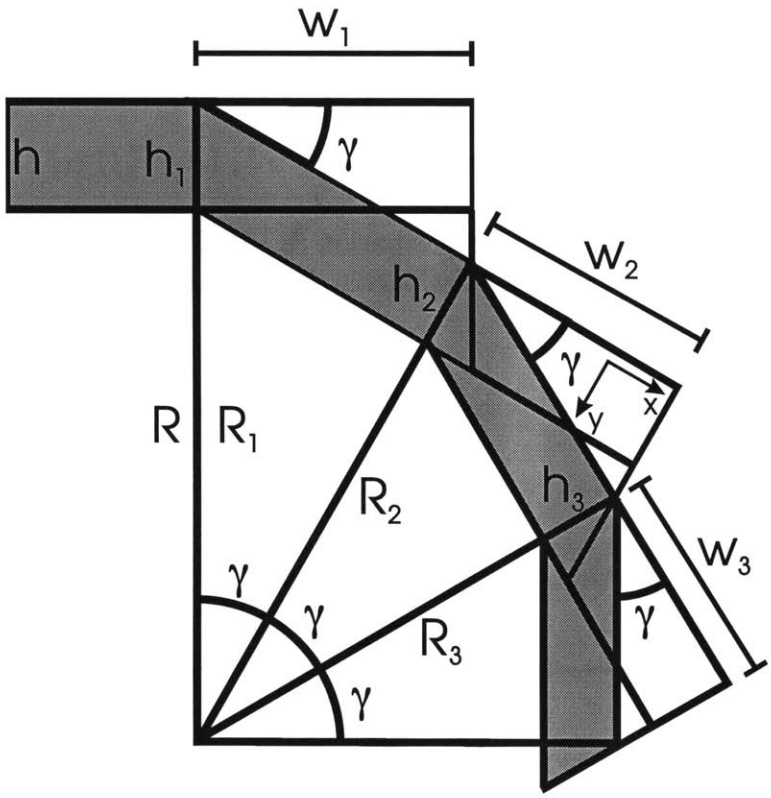

Figure 3-5: Multiple simple shears give in the limit the same geometry as pure bending.

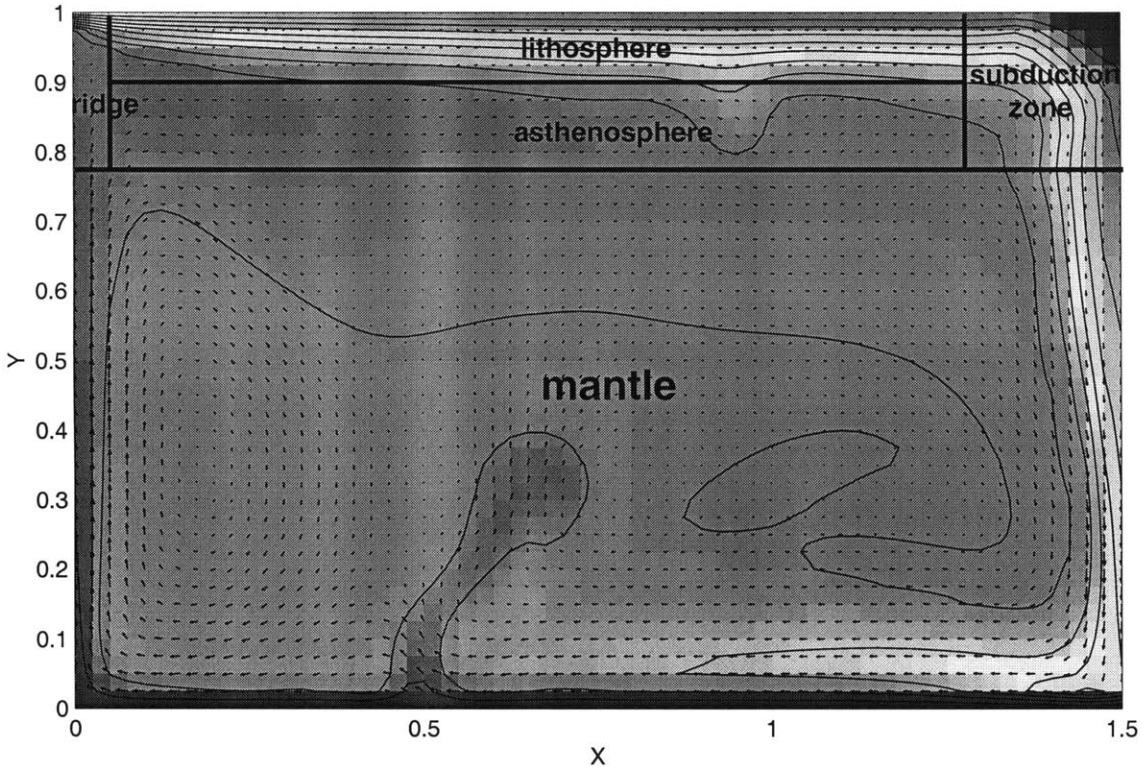

Figure 3-6: Snapshot of mantle convection with subduction dissipation under model with effective lithosphere viscosity $\eta_l = 10000$ and mantle Rayleigh number $Ra_m = 3 \times 10^6$. The various material groups are shown, each of which is characterized by different viscosity laws. Mantle and subduction zone viscosity are temperature-dependent while other regions have constant viscosity. The ridge has viscosity $\eta_r = \eta_m(T = 1)$ and the asthenosphere has a constant low viscosity of $1/10^{th}$ that of the mantle interior. Special velocity boundary conditions in the subduction zone region impose the geometry for subduction, and a rate of plate subduction is specified in order to parameterize the energy dissipation associated with bending deformation

Chapter 4

Discussion: the dissipation equations and boundary layer theory

We can derive an expression for v_p using the energy balance (2.6), equation (2.7), (2.8), and one of the expressions in table (3.1). Thus, for subduction model, we can express the plate velocity as:

$$v_p = \frac{\rho g \alpha \triangle T l_s h_s / \sqrt{\pi}}{C_m \eta_m + 2\eta_l (h_s/R)^3} = \frac{B^{pe} h_s}{B^m + B^l \eta_l h_s^3} \tag{4.1}$$

The plate thickness at the time of subduction and the plate velocity are governed by halfspace cooling of the oceanic lithosphere, which yields the following relationship [*Turcotte and Schubert,* 1982]:

$$h_s = 2\sqrt{\kappa L / v_p} \qquad or \qquad v_p = \frac{4\kappa L}{h_s^2} = \frac{B^p}{h_s^2} \tag{4.2}$$

where L is the distance traveled by the oceanic plate from the ridge to the subduction zone. Combining (4.1) and (4.2) yields an expression for the plate thickness:

$$(B_1 + B_1^i \eta_l) h_s^3 - B_1^{ii} = 0 \tag{4.3}$$

where B_1, B_1^i and B_1^{ii} are constants comprised of R, $\rho, \alpha, \triangle T, l_s, C_m$, and η_m. All future constants with names of this format will be functions of the same kind. After some manipulation, the plate thickness and plate velocity can be written as a function of the mantle Rayleigh number Ra_m as defined in (2.3) [*Conrad,* 2000]:

$$h_s \propto Ra_m^{-\beta} D \qquad and \qquad v_p \propto Ra_m^{2\beta} \kappa / D \tag{4.4}$$

Using (4.4), the total heat flow due to the cooling of oceanic lithosphere can be written as:

$$N = 2D \left(\frac{v_p}{\pi \kappa L} \right)^{(1/2)} \propto Ra_m^{\beta} \tag{4.5}$$

This relationship is analogous to (2.5), which summarizes the theory of parameterized convection. From (4.3) can be shown that a typical value for $\beta = 1/3$. The heat flow N is normalized by dividing by the heat flow from conduction alone and is similar to the Nusselt number (2.5). Thus, for model, theory predicts the general principles of parameterized convection to still hold with energy dissipative subduction zones.

According to equation (3.20), the energy dissipation for mode2 subduction is not proportional to h_s^3 as for model. Instead of (4.3), we now have:

$$\tau_1 \left(B_2 h_s^6 + B_2^i h_s^5 + B_2^{ii} h_s^4 \right) + \tau_0 B_2^{iii} h_s^4 + B_2^{iv} h_s^3 + B_2^v = 0 \tag{4.6}$$

The expression for h_s is thus a 6^{th} order polynomial, which cannot be solved analytically.

For mode3, the plate velocities can be written as:

$$B_3 h_s^4 + B_3^i h_s^3 + \eta_l B_3^{ii} h_s + B_3^{iii} h_s + B_3^{iv} = 0 \tag{4.7}$$

Also this equation does not lead to a straightforward derivation of a powerlaw relationship between the Nusselt number and the Rayleigh number, as was the case for mode1.

Finally, mode4 yields the following expression for the plate velocities:

$$B_4 h_s^3 + \tau_1 \left(B_4^i h_s^4 + B_4^{ii} h_s^3 \right) + \tau_0 B_4^{iii} h_s^3 + B_4^{iv} = 0 \tag{4.8}$$

again, it seems impossible to solve this polynomial equation. If however $\tau_1 = 0$, then (4.8) reduces to:

$$\left(B_4 + \tau_0 B_4^{iii} \right) h_s^3 + B_4^{iv} = 0 \tag{4.9}$$

or, when we write out the B-constants:

$$h_s = \left(\frac{4\kappa L C_m \eta_m}{\rho g \alpha \triangle T l_s / \sqrt{\pi} - \frac{\pi}{2} \tau_0} \right)^{1/3} \tag{4.10}$$

This can be written as:

$$h_s \propto (Ra_m)^{-\beta} \tag{4.11}$$

where it is easily seen that β should have a value of $1/3$, as predicted by standard boundary layer theory. If however:

$$\rho g \alpha \triangle T l_s / \sqrt{\pi} = \frac{\pi}{2} \tau_0, \tag{4.12}$$

or:

$$\frac{2 l_s}{\pi^{3/2}} \rho g \alpha \triangle T = \tau_0^c, \tag{4.13}$$

then the plate thickness h_s becomes infinite, the extreme case of the so called "stagnant lid" mode of convection. For a mantle with $\rho g \alpha = 1 \times 10^6$, and $\triangle T = l_s = 1$, this condition becomes $\tau_0^c = 3.6 \times 10^5$.

Chapter 5

Results

5.1 Modes 1, 2, and 3

In a first step, we repeat the experiments by *Conrad* (2000) for our new configuration of a convection cell without continental lithosphere, but with an asthenosphere. Subduction is initiated by imposing an initial plate velocity of $v_i = 500$ or, for some runs with resistant subduction zones, $v_i = 100$. The mantle is set isothermal with $T_{int} = 0.65$ and Rayleigh number $Ra_m = 10^6$. After typically several thousand time steps, an approximate steady state is reached for the plate thickness h_p, velocity v_p, heat flux N, etc.. These quantities however still oscillate around some mean value. This is exemplified by figure (5-1). As a reminder: we used a slighly modified version of equation (2.15) with $C_l = \frac{1}{3\pi}$ instead of 2, the value obtained by *Conrad and Hager* (1999a). Therefore, the value of the effective lithosphere viscosity $\eta_l = 10000$ used in the model run can be compared with an $\eta_l = \frac{10000}{6\pi} = 530$ viscosity in the work by *Conrad* (2000). For three different runs of the program with different mantle Rayleigh numbers Ra_m, equations (4.4) and(4.5) predict a linear relationship between $log(Ra_m)$ and $log(h_s)$, $log(v_p)$, and $log(N)$ respectively. This is indeed what is observed in figure (5-2). It cannot be the goal of this research to repeat Conrad's research. Now that we know that our model successfully incorporates viscous bending dissipation by subduction zones, we can therefore proceed, and direct the reader to [*Conrad and Hager,* 1999a, & b], and [*Conrad*, 2000] for further information concerning model

subduction.

We already discussed in chapter 4 that contrary to mode1, there is no reason to assume that mode2 and mode3 should show a simple exponential relationship between Ra_m and h_s, v_p, and N. For mode2 subduction, the plate thickness is given by (4.6), a high order polynomial function of the yield stress parameters τ_0 and τ_1. None of the polynomial coefficients can really be ignored, and thus, the equation cannot be analytically solved. Figure (5-3) shows however that for a subduction zone with yield stress parameters $\tau_0 = 1 \times 10^4$ and $\tau_1 = 1 \times 10^7$, we can still see a general trend of increase of the values of v_p and N with Ra_m, while h_p decreases with Ra_m. When the lithosphere strength is increased by raising τ_0 to 1×10^6, the slopes seem to decrease, although the exact value is not clear since the error bars on the data points are significantly larger than before. We can see why this is so on figure (5-4), which represents the time series of v_p, h_p, and the relative importance of bending dissipation for an even stronger subduction zone with $\tau_0 = 1.5 \times 10^6$. The plate velocity is zero for most of the time. This is the so called "stagnant lid" regime, where there is no surface expression of mantle convection, and thus no plate tectonics. This is the mode of convection which is believed to occur on Mars, Mercury, and the Moon [*Moresi and Solomatov,* 1998]. However, after a while, the plate velocity suddenly increases, and over a certain period of time, an Earth like, "mobile lid" regime of mantle convection prevails. The whole sequence of flats and peaks is referred to as the "episodic overturn" regime [*Moresi and Solomatov,* 1998]. This behavior will be discussed more in detail in the next section about brittle behavior under simple shear. We will see that in the special case of mode4 subduction with $\tau_0 = 0$, the transition between "mobile lid, "episodic overturn", and "stagnant lid" can then be treated in a more quantitative way.

Next we discuss mode3 subduction. As for mode2, also here we cannot manage to get a simple power law to explain the data (figure (5-5)). Based of the non-linearity of the problem, we are not allowed to fit a straight line to the data, and indeed the fit does not fall within the error bars of the data points. Still the results of doing the fit make sense, as the slope of N vs. Ra_m, which for mode1 was equal to β, is less

than 1/3. This slope decreases when the subduction zone strength is increased by changing the effective lithosphere viscosity η_l from 5 to 50. The slope of h_p vs. Ra_m is negative, as predicted for model by (4.4). Thus, it seems like although we cannot easily linearize the behavior of mode2 and mode3 suduction, as we could for model, the behavior is still roughly described by the powerlaw relationships (4.4), and (4.5).

5.2 Subduction under mode4

As shown by (4.10), the special case of mode4 subduction with $\tau_0 = 0$ has to yield straight line fits of v_p,h_p, and N vs. Ra_m. This indeed what is observed on figure (5-6) for values of $\tau_0 = 7.5 \times 10^4, 1 \times 10^5$, and 1.25×10^5. For the first two cases, the error bars on the data points are small and the fit is nice. We can see that as the yield stress of the plate increases, the plate velocities decrease, the plate thickness increases, and the heat flow decreases. Also, the slope of the plots, which according to (4.11) equals the parameter value β, decreases away from the value $\beta = 1/3$ predicted by standard boundary layer theory. When we further increase the strength of the subduction zone by raising τ_0 to 1.25×10^5, the error bars on v_p,h_p, and N dramatically increase. This is because τ_0 approaches the critical value given by equation (4.13). This equation gives us the conditions under which a "stagnant lid" is formed and plate tectonics cease to exist. The value of $\tau_0 = 1.25 \times 10^5$ is sufficiently close to the critical yield stress to show some typical brittle behavior. Plate tectonics are still taking place, but not as smooth as for lower plate strengths. The time series of v_p,h_p, and N show a "bumpy" behavior (see figure(5-7)).

When we further increase the yield stress to $\tau_0 = 1.5 \times 10^5$, these characteristics become much more clear, as we can see on figure (5-8). The time series of v_p show the "periodic overturn" regime of mantle convection and thus confirm results of numerical simulations of mantle convection with brittle lithosphere by *Moresi and Solomatov* (1998). Initially, the plate velocity drops to nearly zero. This is the "stagnant lid" regime for which the plate thickness h_p reaches a maximum and the dimensionless heat flow N a minimum. Suddenly (on figure (5-8) at time t=0.018), the plate velocity

dramatically increases to a value of v_p=1000. This marks the beginning of the "mobile lid" regime, which then gradually decays back into a "stagnant lid" situation again. This cycle repeats with a periodicity T=0.015. The "episodic overturn" regime has been proposed as the possible mode of mantle convection on Venus, where the friction coefficient of the lithosphere is assumed to be high due to the dry conditions (no oceans). It is nicely displayed in figure (5-9).

The next obvious step is further increasing τ_0 to a value greater than the critical value $\tau_0^c = 3.6 \times 10^5$. Figure (5-10) illustrates such a run for which the "stagnant lid" regime is the only one possible. The whole sequence of "mobile lid", "episodic overturn", and "stagnant lid" that was just described for mode4 subduction was also observed for mode2. Hence, it seems that this is a feature which is characteristic for brittle subduction zones.

5.3 Is boundary layer still valid with dissipative subduction zones?

The careful reader might have noticed that on figure (5-2), the values of β calculated from the slopes of v_p, h_p, and N vs. Ra_m are not equal to each other, although the data points do fit a straight line very well, as predicted by (4.11). This suggests that there might be something wrong with the basic assumptions of boundary layer theory which led to the prediction of a consistent parameterization through β with equation (4.5). Indeed, equation (4.2) implies that the product $v_p h_p^2$ should be constant at a value of $C\kappa L$. With values of $\kappa = 1$, L=1, and C=4, as given by [*Conrad and Hager,* 1999a], this leads to $v_p h_p^2 = 4$. Nevertheless, figure (5-11) shows that this is not the case and that $v_p h_p^2$ in general is smaller than 4. $v_p h_p^2$ is however only weakly dependent on Ra_m so that we can consider the value of B^p in (4.2) as constant in a first approximation, and the derivations in Chapter 4 still hold. Except for mode1 subduction, also mode2, 3, and 4 are plotted. The weak dependence of $v_p h_p^2$ on Ra_m can be an effect of the presence of an asthenosphere, which keeps the plate thickness

fixed at a certain value, so that the lithosphere thickness can no longer be described by an error function, which was one of the assumptions behind equation (4.2). This could explain why the values of β determined from the plots of v_p and N vs. Ra_m seem to be more consistent with each other that the plots of h_p vs. Ra_m. There can also be numerical artefacts of the discretization which would disappear if the grid density was increased.

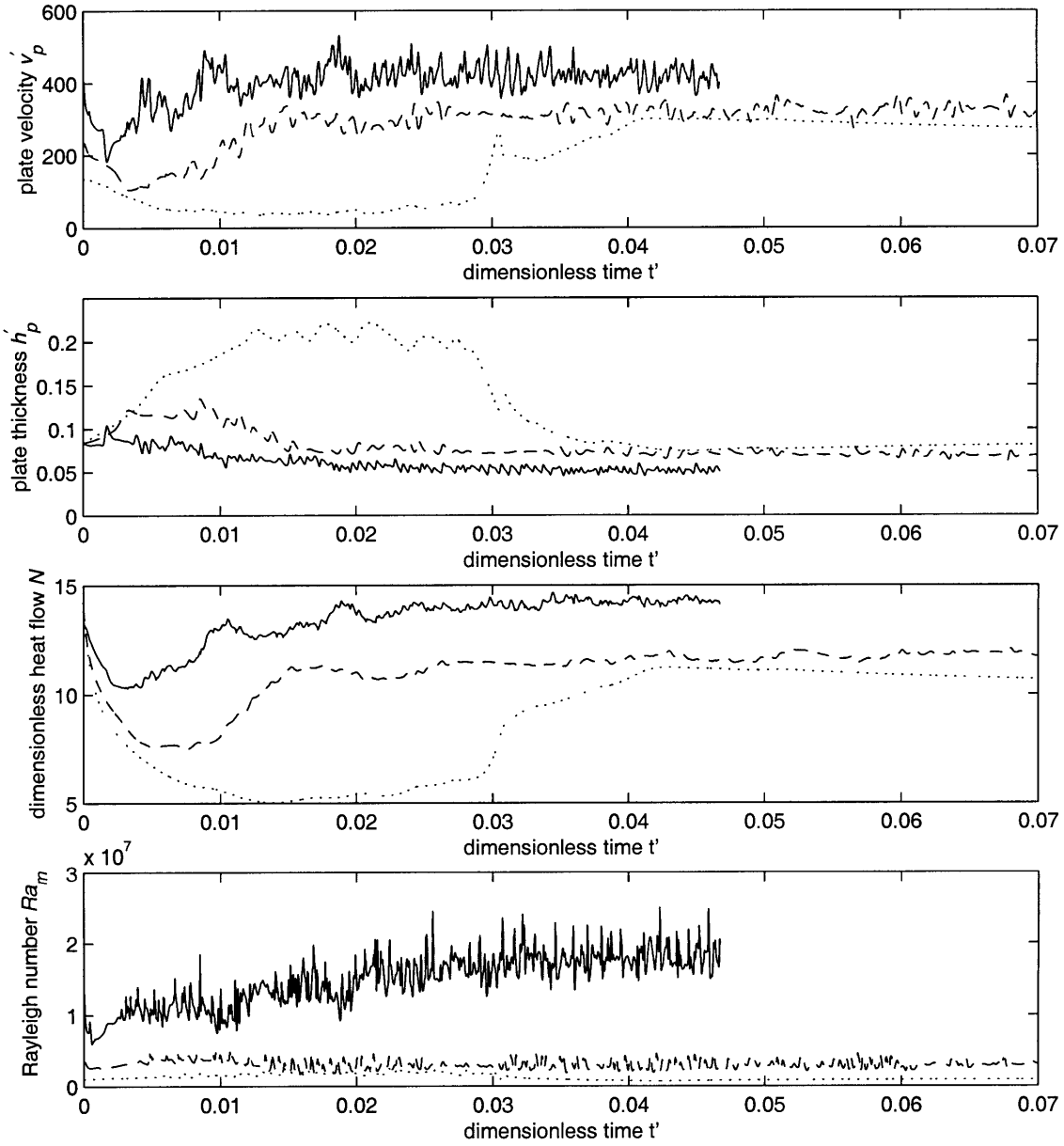

Figure 5-1: Evolution of various non-dimensional subduction parameters with non-dimensional time for model subduction with effective lithosphere viscosity $\eta'_l = 1 \times 10^4$. Solid line: initial mantle viscosity $(\eta'_m)_0 = 1.25\times10^{-2}$, dashed line: $(\eta'_m)_0 = 4.2\times10^{-2}$, dotted line: $(\eta'_m)_0 = 1.25\times10^{-1}$

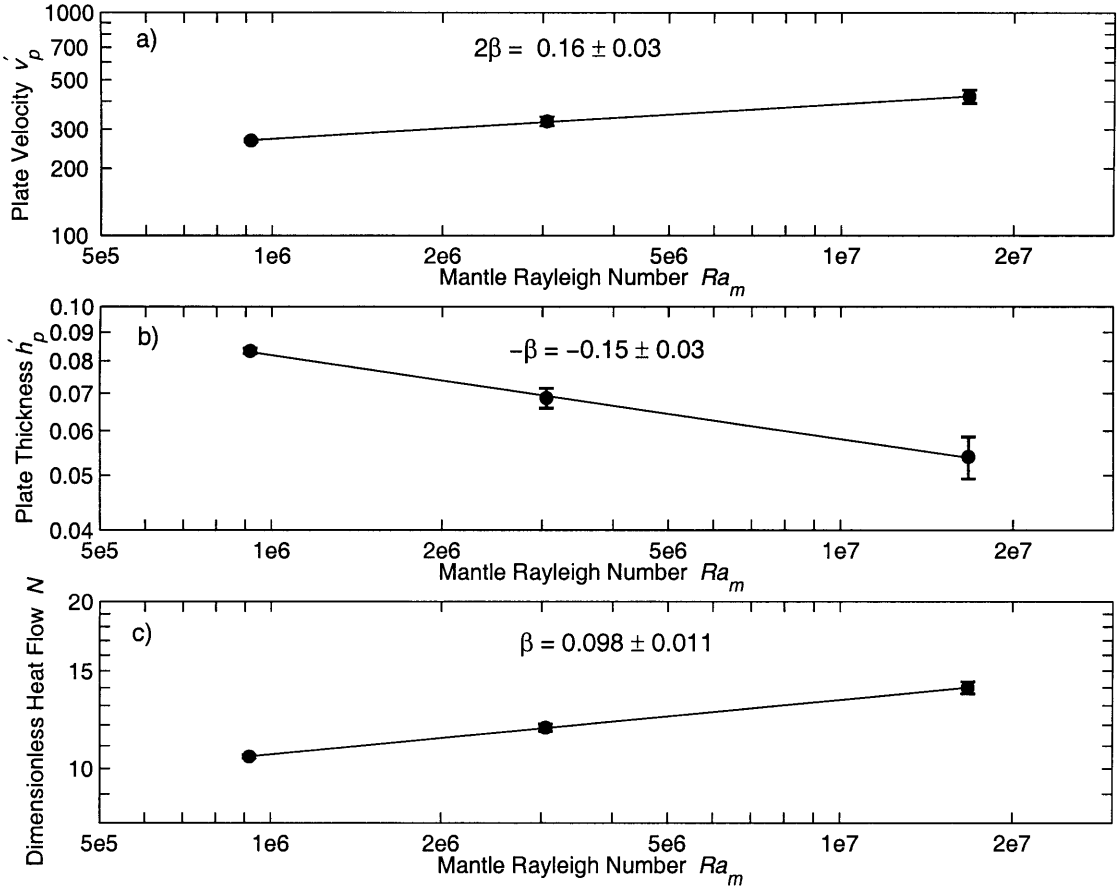

Figure 5-2: Log-log plots for model subduction with effective lithosphere viscosity $\eta'_l = 1 \times 10^4$ showing the dependence of (a) plate velocity v'_p, (b) plate thickness h'_p, and (c) total heat flow N on the mantle Rayleigh number Ra_m. According to (4.4), v'_p should depend on $Ra_m^{2\beta}$, and h'_p on $Ra_m^{-\beta}$, while according to (4.5), N should be proportional to Ra_m^{β}. If boundary layer theory applies, we expect a value for $\beta = 1/3$. We observe $\beta < 1/3$ for this run, which represents a relatively resistant subduction zone, and includes an asthenosphere.

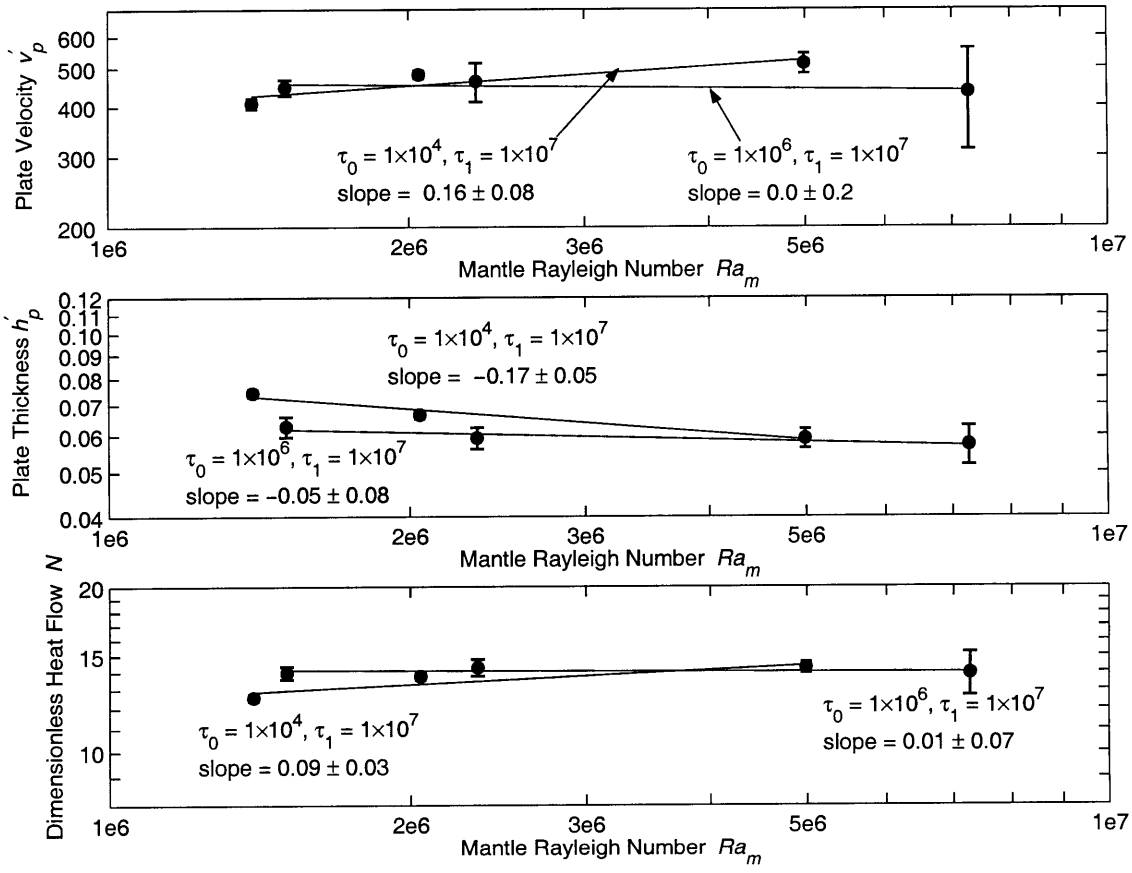

Figure 5-3: mode2 subduction: strictly speaking, we are not allowed to fit a straight line to the data, and the fit does not fall within the error bars of the data points. Still the predictions of the standard theory of parameterized convection seem to remain valid for the weak subduction zone with yield stress parameter $\tau_0 = 1 \times 10^4$. The slope of the plots of v_p' and N vs. Ra_m are positive, while the slope of h_p' vs. Ra_m is negative. For the stronger subduction zone ($\tau_0 = 1 \times 10^6$), the error bars on the data points are larger and the slope of the regression is less clear. This is due to some typical brittle behavior which is more thoroughly explored for mode4 subduction, as shown in figures (5-6) through (5-10).

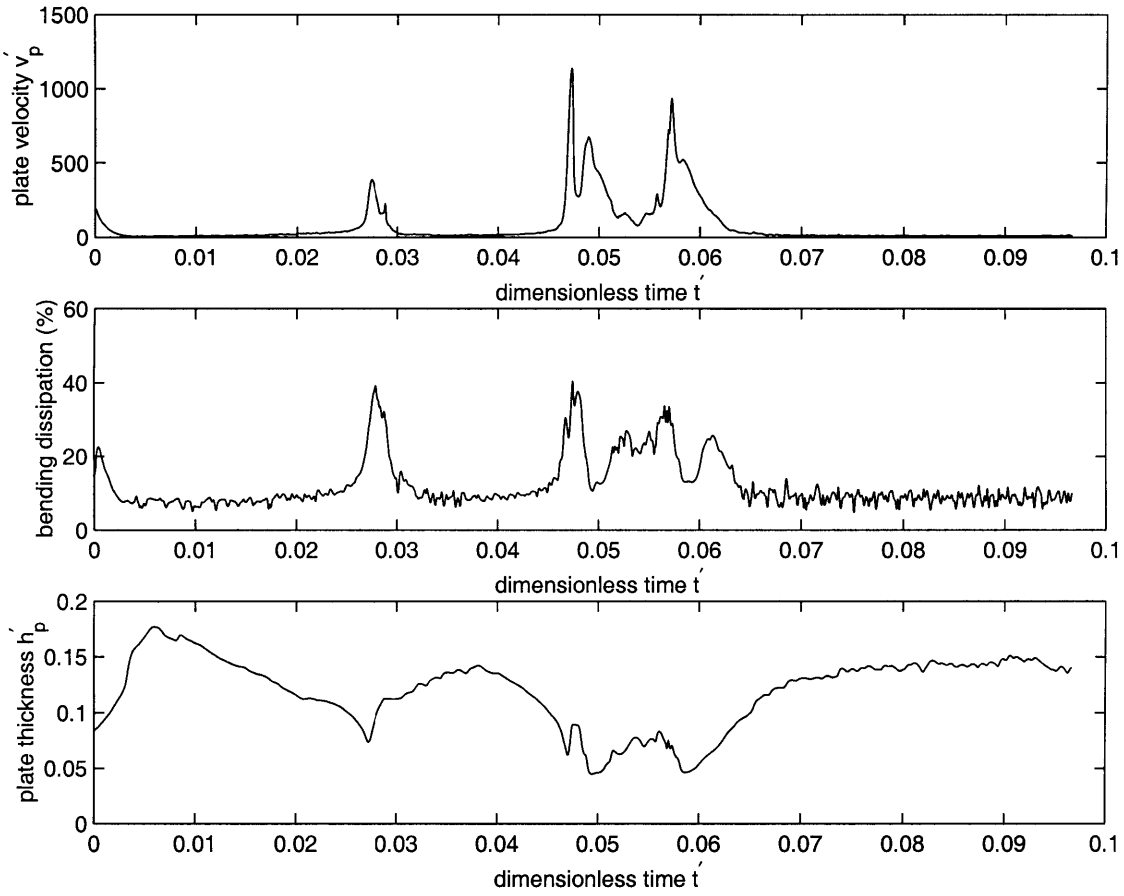

Figure 5-4: mode2 subduction: for a strong subduction zone with $\tau_0 = 1.5 \times 10^6$, mantle convection no longer yields smooth plate tectonics, but in an "periodic overturn" regime, switches between a "stagnant lid" regime -where the plate velocities are zero and the plates freeze- and the "mobile lid" regime, where plate tectonics dominate. This cyclic and catastrophic mode of mantle convection has been proposed as occuring on Venus, where yield stresses are high due to the dry conditions prevailing.

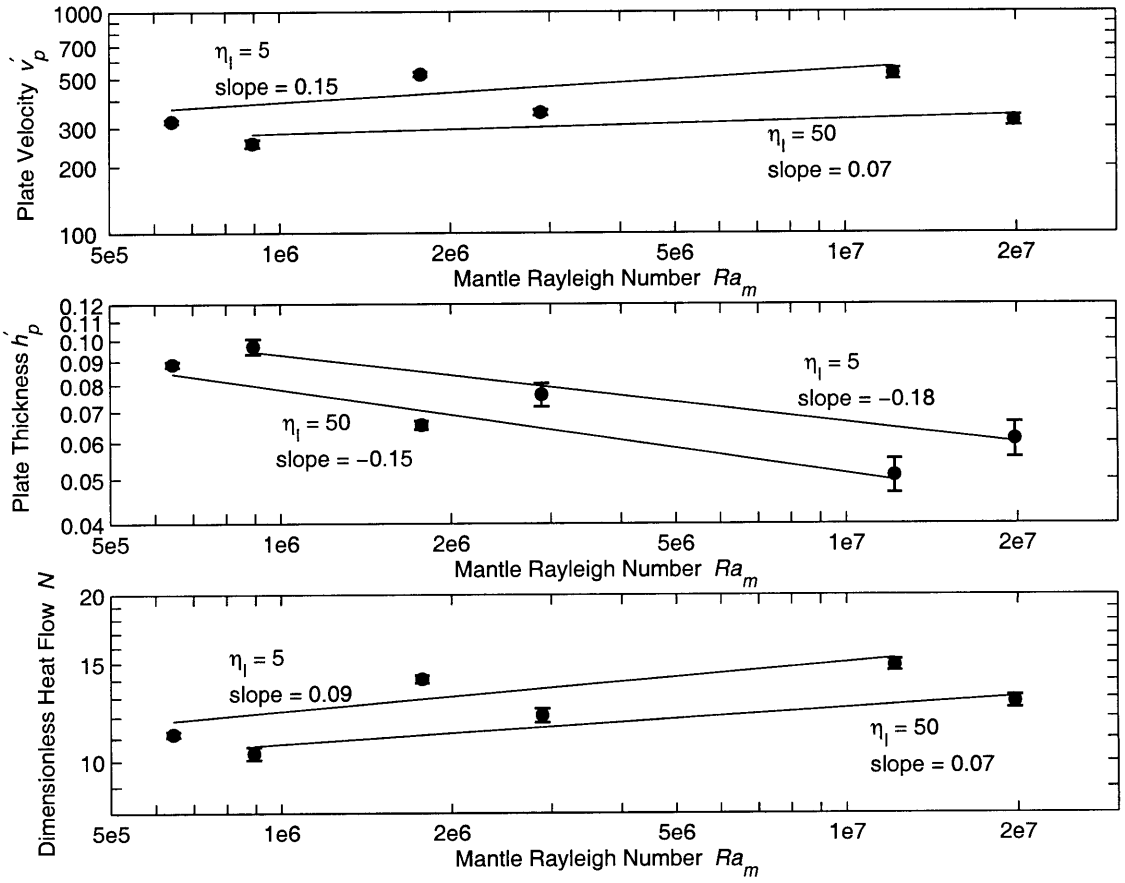

Figure 5-5: mode3 subduction: as for mode2, we are not really allowed to fit a straight line to the data, and the fit does not fall within the error bars of the data points. Still the results of doing the fit make sense, as the slope of v'_p and N vs. Ra_m, which for model was equal to β, is less than 1/3. This slope decreases when the subduction zone strength is increased by changing the effective lithosphere viscosity η_l from 5 to 50.

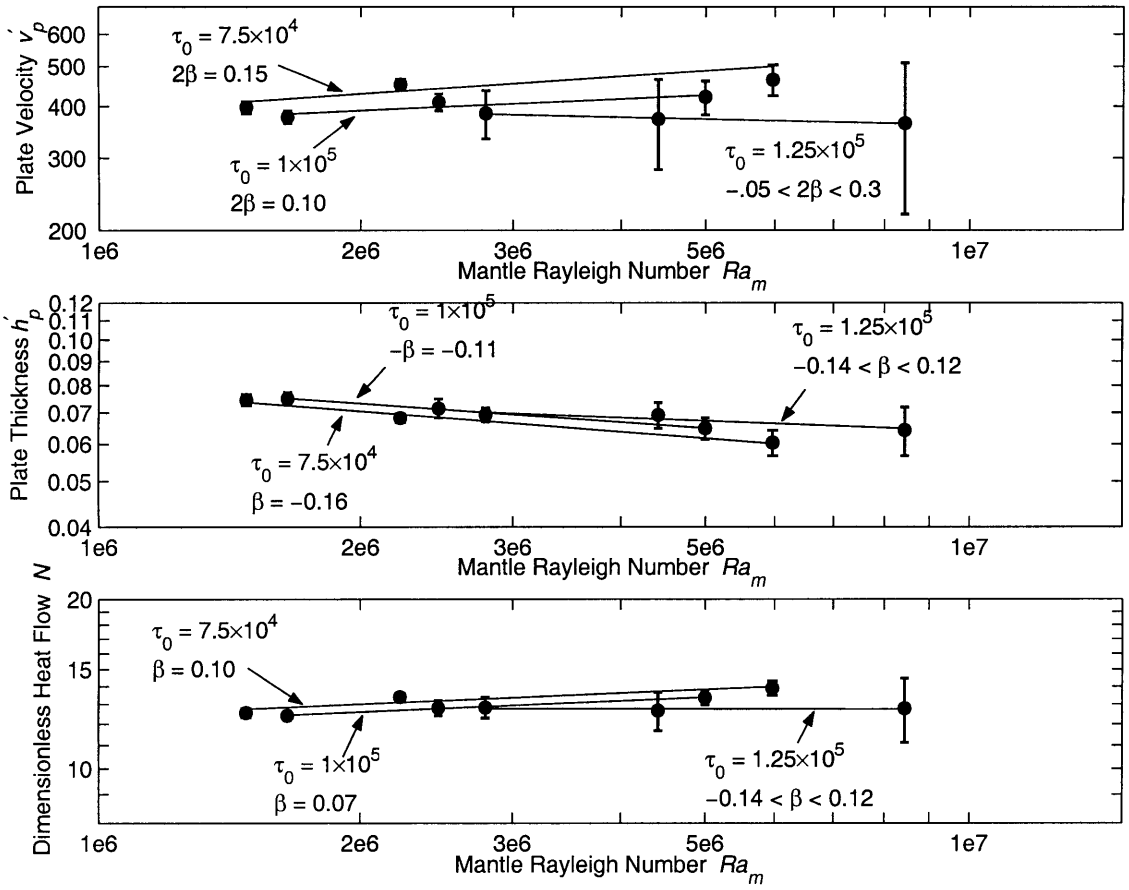

Figure 5-6: mode4 subduction with τ_1=0: for values of the yield stress $\tau_0 = 7.5 \times 10^4$ and 1×10^5, the error bars on the data points are small and the fit is nice. We can see that as the yield stress of the plate increases, the plate velocities decrease, the plate thickness increases, and the heat flow decreases. Also, the slope of the log-log plots, which according to (4.11) equal the parameter value β, decrease away from the value $\beta = 1/3$ predicted by standard boundary layer theory. When we further increase the strength of the subduction zone by raising τ_0 to 1.25×10^5, the error bars on v'_p,h'_p, and N dramatically increase. This is because τ_0 approaches the critical value given by equation (4.13). This equation gives us the conditions under which a "stagnant lid" is formed and plate tectonics cease to exist.

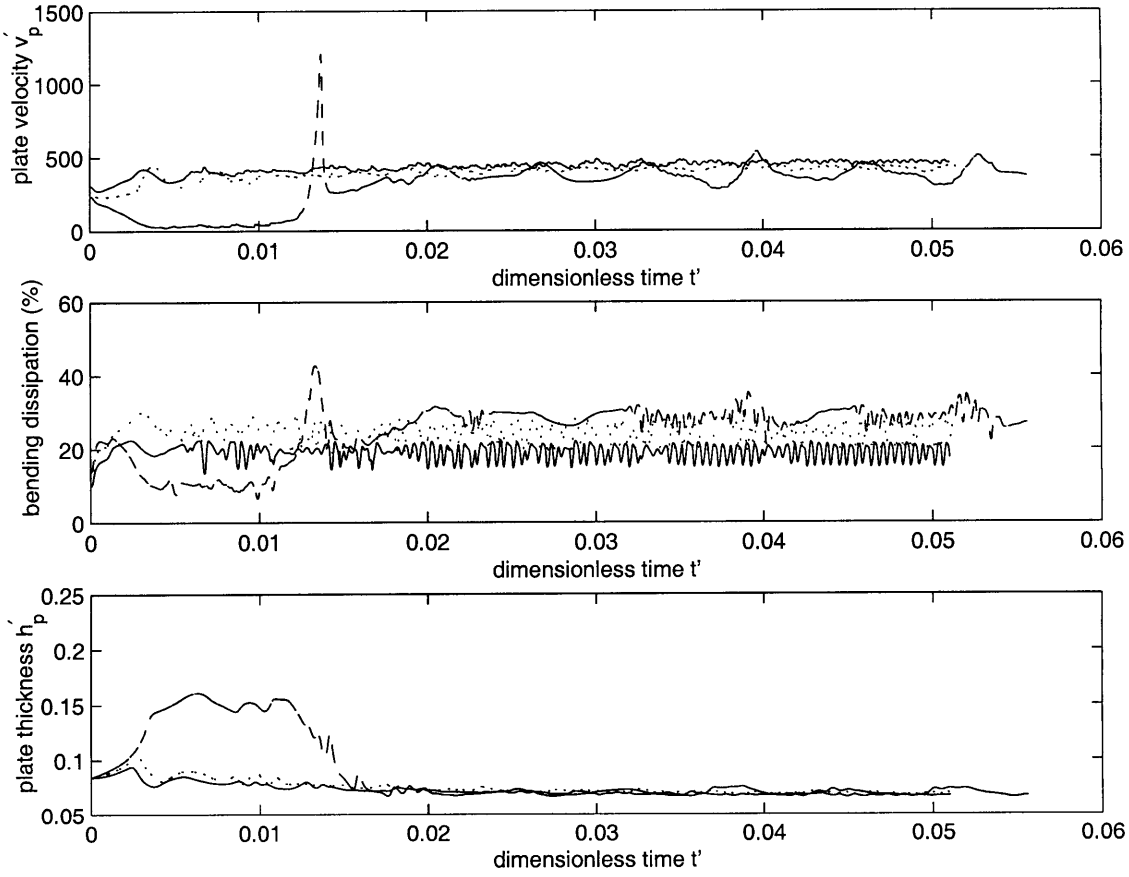

Figure 5-7: mode4 subduction with τ_1=0: evolution with time of the plate velocity v_p', the fraction of the total energy dissipation associated with subduction dissipation, and the plate thickness h_p'. Results are shown for three subducting slabs with η_l' of 7.5×10^4 (solid line), 1×10^5 (dotted line), and 1.25×10^5 (dashed line). The subduction zone with $\tau_0 = 1.25 \times 10^5$ shows some features of brittle behavior which will become more clear for even higher τ_0 in figure (5-8). Ra_m is 2.2×10^6, 2.35×10^6, and 2.7×10^6 respectively.

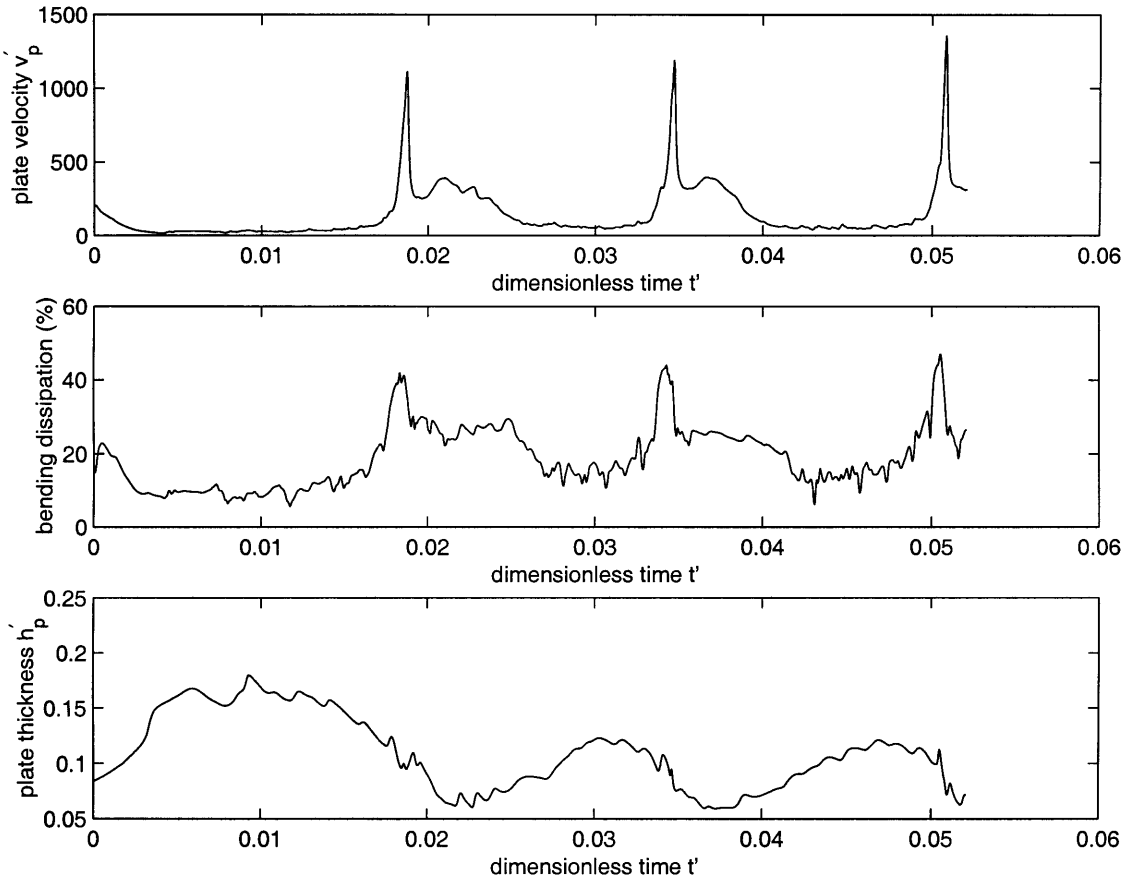

Figure 5-8: mode4 subduction with $\tau_1 = 0$ and $\tau_0 = 1.5 \times 10^5$. τ_0 is sufficiently close to the critical value of $\tau_0^c = 3.6 \times 10^5$ to develop a so called "periodic overturn" regime of mantle convection. Initially, the plate velocities drop to nearly zero. This is the "stagnant lid" regime for which the plate thickness h'_p reaches a maximum and the dimensionless heat flow N a minimum. Suddenly (at time t'=0.018), the plate velocity dramatically increases to a value of v'_p=1000. This marks the beginning of the "mobile lid" regime, which gradually decays back into a "stagnant lid" situation. This cycle repeats with a periodicity T'=0.015.

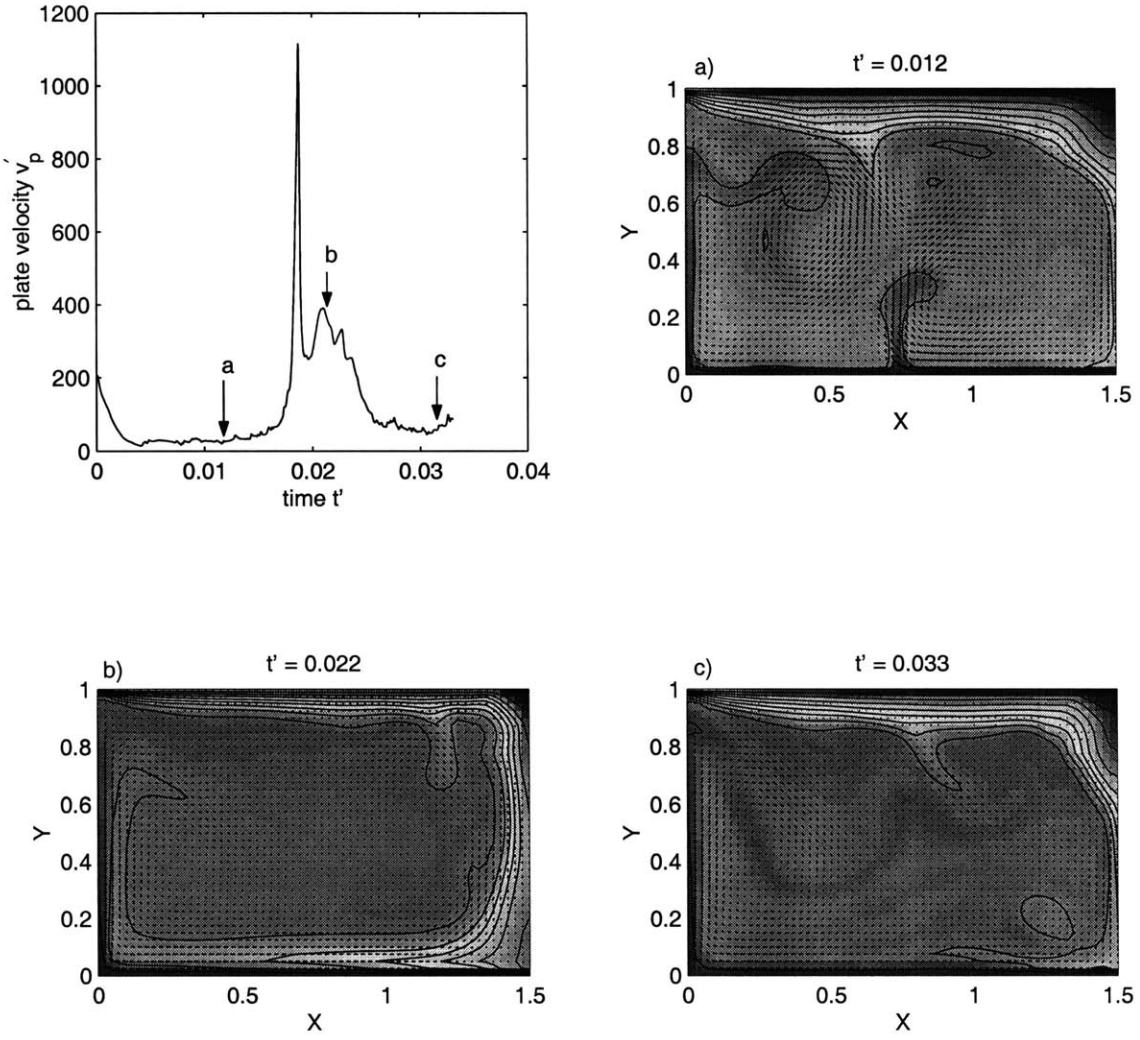

Figure 5-9: The first plot shows the first cycle of the v_p' time series for mode4 subduction with $\tau_1 = 0$ and $\tau_0 = 1.5 \times 10^5$. The next three plots are snapshots of the temperature (contours) and velocity field (vectors) at certain time steps. They exemplify the "periodic overturn" regime of mantle convection. (a) Initially the plate velocity drops to almost zero to form a "stagnant lid" regime of mantle convection. (b) After a sharp peak in v_p', plate tectonics resume, this is the "mobile lid" regime. (c) The plate velocity gradually drops again to form a new "stagnant lid".

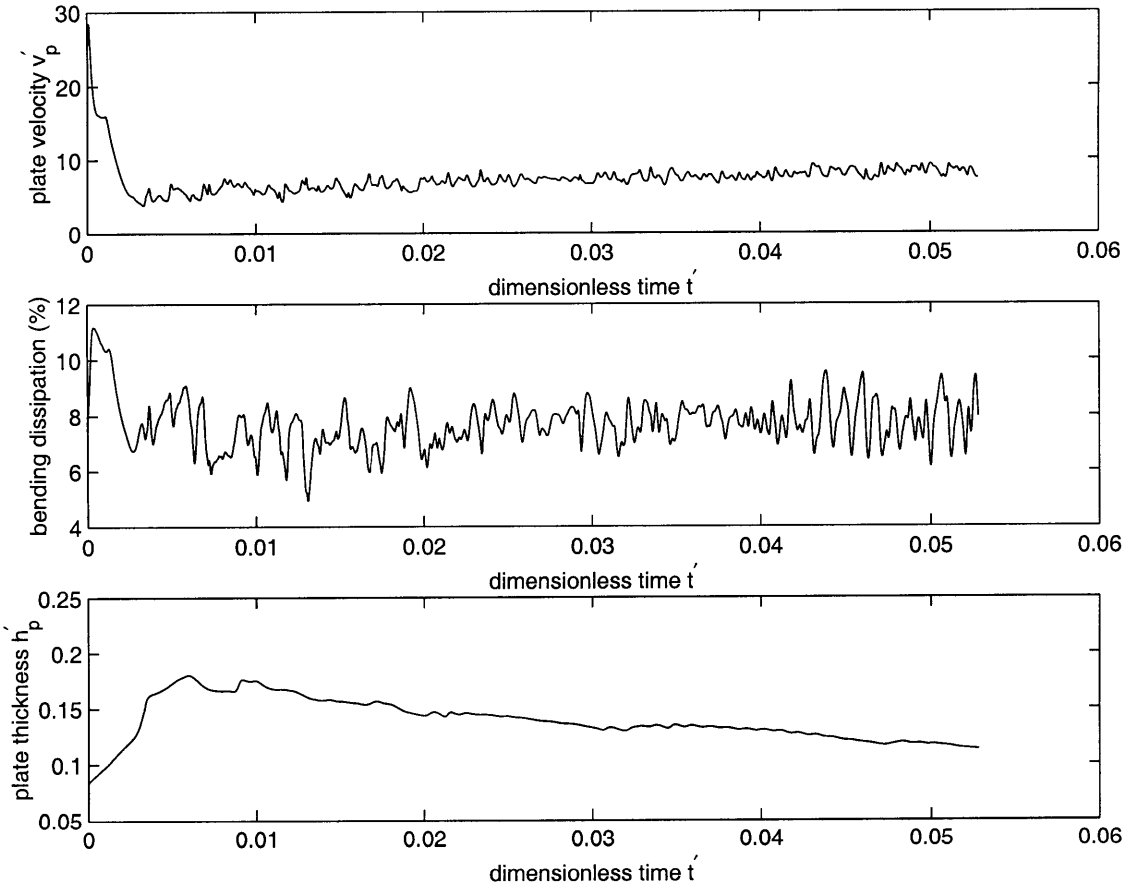

Figure 5-10: mode4 subduction with $\tau_1 = 0$ and $\tau_0 = 1.5 \times 10^5$: when the yield stress parameter τ_0 exceeds the critical value τ_0^c, a "stagnant lid" develops.

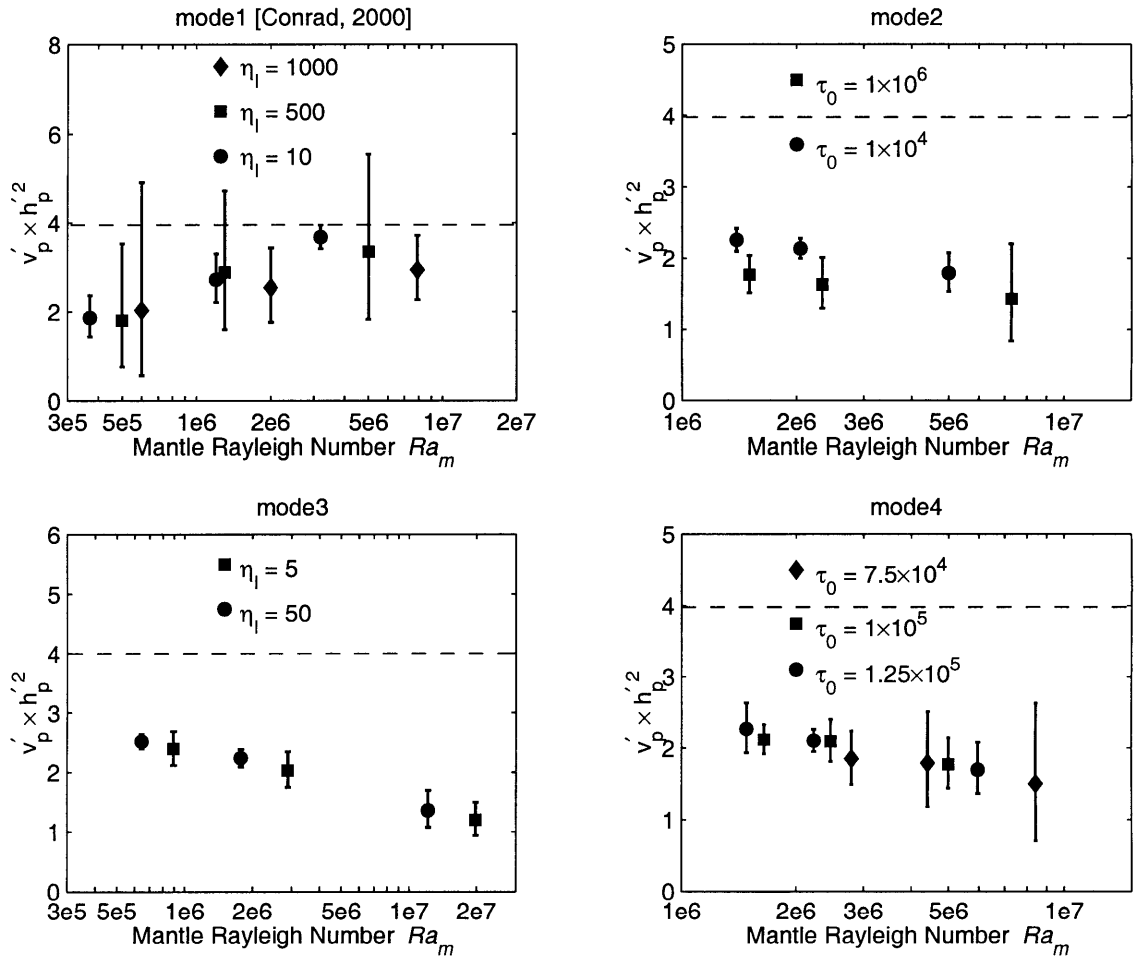

Figure 5-11: If boundary layer theory applies to mantle convection with subduction zones, then equation (4.2) predicts the product $v_p' h_p'^2$ to be constant and equal to $C\kappa L$, which is proposed by [*Conrad and Hager*, 1999a] to be 4. These plots show that this is not true and that $v_p' h_p'^2$ in general is smaller than 4. $v_p' h_p'^2$ is however only weakly dependent on Ra_m so that we can consider the value of B^p in (4.2) as constant in a first approximation, and the derivations in Chapter 4 still hold. The data for model subduction are taken form [*Conrad,* 2000] with no asthenosphere in the case of $\eta_l = 10$,,and $\eta_l = 500$, but including an asthenosphere for $\eta_l = 1000$. The dashed line indicates the predicted value of $v_p' h_p'^2 = 4$ from [*Conrad and Hager*, 1999a].

Chapter 6

Conclusions and future research

6.1 Conclusions

We have successfully explored the effects of various modes of energy dissipation at subduction zones on mantle convection. Four different ways of deforming an oceanic slab were parameterized in a finite element representation of a mantle with subduction zone which also includes an asthenosphere and a ridge.

Viscous energy dissipation was modeled for both pure bending strain and simple shear. Two regimes of mantle convection could be delimited. For weak subduction zones, with low effective viscosity, plate-like surface motions are produced in a "mobile lid" regime of mantle convection even if the bending deformation associated with subduction dissipates a significant portion of the mantle's total convective energy. In this case, the plate velocities slow down significantly. In the case of viscous bending deformation, the powerlaw relationship of parameterized convection $N \propto Ra^{\beta}$ seems to still hold, with a value of β which is less than the value of $1/3$ predicted by standard boundary layer theory. However, the product $v_p \times h_p^2$ is lower than the value of 4 necessary for boundary layer theory to be valid. Still, $v_p \times h_p^2$ is approximately constant so that the general powerlaw relationships between the plate velocity v_p, the plate thickness h_p, the Nusselt number N and the Rayleigh number Ra_m still hold. For viscous dissipation under simple shear, these powerlaw relationships cannot be derived analytically, although numerical experiments show that they are still valid as

a first approximation.

Also for brittle behavior expressions were derived for the energy dissipation associated with the subduction of oceanic lithosphere under both pure bending and simple shear. In general, we cannot derive simple powerlaw expressions between v_p, h_p, N, and Ra_m for these modes. In the special case of a non-depth dependent yield stress, however, we can, and simulations show that in the "mobile lid" regime the data indeed fit a straight line on a log-log plot. Where viscous behavior could yield two regimes of mantle convection -the "mobile lid", and the "stagnant lid"-, brittle behavior also features a third, intermediate one: the "episodic overturn" regime. A state of "episodic overturn" is reached when the yield stress approximates a critical value, beyond which a "stagnant lid" develops.

As a general rule, we can say that including an energy dissipative subduction zone in a model for convection of the mantle decreases the strength of the coupling between the Rayleigh number and the Nusselt number, and between the Rayleigh number and the plate velocity. Therefore, plate velocities do not change as much with time as for standard boundary layer theory. This allows the Urey ratio to be less than 0.85, and yields a more realistic reconstruction of the thermal history of the Earth.

6.2 Future research

As was outlined in the Introduction, there are some discrepancies between the reconstruction of the thermal history of the Earth based on standard boundary layer theory and the observed heat flow as measured at the Earth's surface. In short, boundary layer theory predicts a Urey ration of 0.85, which would require about ten times as much heat production as inferred from the radioactive element content of MORBs. There are two ways by which we can solve this problem. The first way is to lower the Urey ratio allowed by mantle convection. This is what the research here presented was basically about. A second way of solving the contradictions is by allowing more radioactive heat production in the mantle than measured in MORBs. This can be done by incorporating a compositionally distinct layer in the deep mantle [*Kellogg et*

al., 1999]. It would be interesting to combine the two approaches in one finite element representation of the mantle, and see if this indeed results in a realistic reconstruction of the thermal history of the Earth.

Appendix A

Non-dimensionalizations, boundary conditions, and initial conditions

Non-dimensionalizations	
Viscosity	$\eta' = \frac{\eta}{\eta_0}$
Distance	$z' = \frac{z}{D}$
Time	$t' = t\frac{\kappa}{D^2}$
Velocity	$v' = v\frac{D}{\kappa}$
Temperature	$T' = \frac{T-T_s}{T_b-T_s}$
Non depth dependent yield stress parameter	$\tau_0 = \frac{c_0 d^2}{\kappa\eta_0}$
Depth dependent yield stress parameter	$\tau_1 = \frac{\mu Ra_0}{\alpha\Delta T}$

Representative values used for non-dimensionalizations	
Reference viscosity	$\eta_0 = \eta_m(Ra_m = 10^6)$
Activation energy	$E_a = 100\ kJmol^{-1}$
Surface temperature	$T_s = 0^oC$
Temperature at CMB	$T_b = 2000^oC$
Initial interior temperature	(*) see discussion below
Temperature at bottom of lithosphere	$T_p = 1100^oC$
Maximum viscosity	$\eta'_{max} = 1000$
Density of the mantle	$\rho_m = 3300\ kgm^{-3}$
Thermal expansivity	$\alpha = 3 \times 10^{-5}K^{-1}$
Thermal diffusivity	$\kappa = 10^{-6}m^2s^{-1}$
Depth of mantle	$D = 2500\ km$
Viscosity structure	
Mantle	$\eta'_m(T') = \eta'_m(T'_{int})exp(\frac{E_a}{RT'\Delta T} - \frac{E_a}{RT'_{int}\Delta T})$
Subduction zone	$\eta'_{sz}(T') = \eta'_m(T')$
Ridge	$\eta'_r = \eta'_m(T' = 1)$
Asthenosphere	$\eta'_{sz}(T') = \eta'_m(T'_{int})/10$
Velocity boundary conditions	
Top and bottom	free slip
Sides	flow through
Initial forcing velocity of subduction	$v'_0 = 100\ or\ 500$

(*) To initiate subduction, we first impose a constant dimensionless subduction velocity of v'_i=500 on an initially isothermal mantle with non-dimensional temperature T'_{int}=0.65 and Rayleigh number $Ra_m = 10^6$. The top of the mantle cools down and forms a lithosphere which subducts into the mantle, forming a slab. After a while, the temperature field ceases to change significantly with time. This temperature field is then used as the initial condition in all further runs.

References

Chandrasekhar, S., *Hydrodynamic and hydromagnetic stability*, Oxford University Press, Oxford, 1961.

Christensen, U., Thermal evolution models for the earth, *Journ. Geophys. Res., 90,* 2995-3007, 1985.

Conrad, C. P., *Effects of lithospheric strength on convection in the earth's mantle*, (Ph.D. thesis). Cambridge: Massachusetts Institute of Technology ,2000.

Conrad, C. P., and B. H. Hager, The effects of plate bending and fault strength at subduction zones on plate dynamics, *Journ. Geophys. Res., 104,* 17551-17571, 1999a.

Conrad, C. P., and B. H. Hager, The thermal evolution of an Earth with strong subduction zones, *Geophys. J. Int., 26,* 3041-3044, 1999b.

Davies, G. F., Thermal histories of convective Earth models and constraints on radiogenic heat production in the earth, *Journ. Geophys. Res., 85,* 2517-2530, 1980.

Hughes, T. J. R., *The Finite Element Method,* Prentice-Hall, Englewood Cliffs, NJ, 1987.

Jochem, K. P., A. W. Hofmann, E. Ito, H. M. Seufert, and W. M. White, K, U and Th in mid-ocean ridge basalt glasses and heat production, K/U and K/Rb in the mantle, *Nature, 306,* 431-436, 1983.

Kellogg, L. H., B. H. Hager, and R. D. van der Hilst, Compositional stratification in the deep mantle, *Science, 283,* 1881-1884, 1999.

King, S. D., A. Raefsky, and B. H. Hager, ConMan: vectorizing a finite element code for incompressible two-dimensional convection in the Earth's mantle, *Phys. Earth Planet. Inter., 59,* 195-207, 1990.

Kohlstedt, D. L., B. Evans, and S. J. Mackwell, Strength of the lithosphere: Constraints imposed by laboratory experiments, *Journ. Geophys. Res., 100,* 17587-

17602, 1995.

Moresi, L., and V. Solomatov, Mantle convection with a brittle lithosphere: Thoughts on the global tectonic styles of the Earth and Venus, *Geophys. J. Int., 133,* 669-682, 1998.

Nikishkov, G. P., Introduction to the finite element method. Lecture notes, University of Aizu, 1998. http://care.seas.ucla.edu/niki/feminstr/introfem/introfem.html

Richter, F. M., Regionalized models for the thermal evolution of the earth, *Earth Planet. Sci. Lett., 68,* 471-484, 1984.

Temam, R., *Navier-Stokes equations: theory and numerical analysis,* North Holland, Amsterdam, 148-156.

Turcotte, D. L., and E. R. Oxburgh, Finite amplitude convective cells and continental drift, *J. Fluid Mech., 28*, 29-42, 1967.

Turcotte, D. L. and G. Schubert, *Geodynamics,* John Wiley and Sons, New York, 1982.